# Viability assessment of commercially owned battery energy storage systems and demand side response in a medium voltage grid.

by

## Patrick Breedveld

to obtain the degree of Master of Science
at the Delft University of Technology,
to be defended publicly on Thursday August 31, 2023 at 9:00 AM.

An electronic version of this thesis is available at `http://repository.tudelft.nl/`.

TU Delft

STEDIN.NET

# Abstract

In response to the urgent need for sustainable energy solutions and climate change mitigation, international agreements such as the Paris Agreement have been instrumental in advocating reduced greenhouse gas emissions. As the world shifts towards renewable energy sources and electrification, there arises a heightened challenge of increased congestion and a greater demand for flexibility within electrical networks. Batteries emerge as a crucial source of added flexibility and congestion relief. However, these commercially owned batteries are not obliged to assist with grid congestion, possibly focusing solely on energy arbitrage pursuits for example.

This thesis undertakes an exploration of optimizing the efficiency of energy arbitrage batteries by repositioning them to alleviate congestion. Additionally, it delves into the divergence between preferred battery locations for grid operators and battery owners. A comparative analysis is performed among energy arbitrage batteries, congestion relief batteries, and traditional reinforcements. These aspects are evaluated in terms of their contribution to grid flexibility, congestion relief, and load curtailment requirements. The study is conducted using a medium voltage network of a region in the North Rotterdam as a case study.

The investigation involves the creation of a linear programming day-ahead market model and a linear programming energy arbitrage battery model. The day-ahead market model generates a price signal that guides the energy arbitrage battery's charging and discharging decisions for profit maximization. Load and generation forecasts are provided by Stedin for the case study. A Powerfactory model simulates the effect of a congestion relief battery capacity on congestion. Through a heuristic algorithm, the optimal location and size of the energy arbitrage battery capacity are determined.

By analyzing these scenarios, the study unveils the positive impact of strategically positioned energy arbitrage batteries that align discharge timing with congestion patterns. The study also highlights the significance of positioning batteries at the deepest points of radial lines to maximize benefits, even though these locations may diverge from battery owner preferences, such as solar farm sites. Interestingly, the addition of energy arbitrage batteries to these solar farm sites can exacerbate congestion due to their relatively low congestion levels. A comparative evaluation reveals that batteries surpass traditional grid reinforcement in enhancing flexibility, with congestion relief batteries outperforming energy arbitrage batteries in alleviating congestion. With the energy arbitrage battery being able to reduce congestion by 27% and the congestion relief batteries being able to reduce it by 94% with the same amount of installed capacity. Energy arbitrage scenarios may necessitate load curtailment to address congestion challenges, they may not independently resolve all congestion.

In conclusion, while energy arbitrage batteries show promise in addressing congestion, their effectiveness depends on synergistic technologies and further refinement. Future research avenues may explore enhanced market models, extended predictive analyses, and intricate hybrid strategies to tackle congestion relief, considering the intricate complexities introduced by diverse network topologies.

# Acknowledgements

I am deeply grateful to all those who have supported me throughout the journey of completing this thesis. Their guidance, encouragement, and invaluable insights have helped me greatly in making this thesis. I would like to express my sincere gratitude to my primary supervisor, Dr. ir. Milos Cvetkovic, from the Delft University of Technology. His expertise in the field has been instrumental in guiding me through the research process. Additionally, I am also thankful to Prof. dr. Peter Palensky and Dr. ir. Laura Ramirez Elizondo for agreeing to be on the thesis committee.

I am equally indebted to my co-supervisors, Bart Kers and Nuran Cihangir Martin, from Stedin. Their practical experience and industry insights have provided a real-world context to my research. Their willingness to share their expertise and to engage in constructive discussions have expanded my horizons and deepened my understanding of the subject matter.

I extend my heartfelt thanks to the entire team at Stedin for their cooperation and support. Their willingness to share data, provide resources, and engage in meaningful conversations has been invaluable to the success of this research. The collaborative environment fostered by the Stedin team has been an inspiration and a driving force behind the completion of this thesis.

My family and friends deserve special recognition for their unwavering support and encouragement. Their belief in me helped lift my spirits and motivate me.

Lastly, I would like to express my gratitude to the broader academic community for their contributions to the body of knowledge in this field. Their works have served as both a foundation and a source of inspiration for this thesis. With the insights derived from this research, I hope to contribute to the ongoing efforts towards a cleaner energy transition and a more sustainable global future.

*Patrick Breedveld*
*Delft, August 2023*

# Contents

# Nomenclature

*If a nomenclature is required, a simple template can be found below for convenience. Feel free to use, adapt or completely remove.*

## Abbreviations

| Abbreviation | Definition |
| --- | --- |
| COP21 | 21st Conference Of Parties |
| DSO | Distribution System Operator |
| TSO | Transmission System Operator |
| QDS | Quasi Dynamic Simulation |
| PTDF | Power Transfer Distribution Factor |
| DAM | Day Ahead Market |
| MCP | Market Clearing Price |
| BRP | Balancing Responsible Party |
| FCR | Frequency Containment Reserves |
| FRR | Frequency Restoration Reserve |
| SW | Social Welfare |
| LCOE | Levelized Cost of Energy |
| WACC | Weighted Average Cost of Capital |
| II3050 | Integral Infrastructure-outlook 2030-2050 |
| LP | Linear Programming |
| MILP | Mixed Interger Linear Programming |
| SOC | State Of Charge |
| SETIAM | Stedin Energy Transition Impact Assessment Model |
| HV | High Voltage |
| MV | Medium Voltage |
| LV | Low Voltage |
| PTDF | Power Transfer Distribution Factors |
| AM | Analytical Methods |
| MP | Mathematical Programming |
| PILC | Paper-Insulated Lead-Covered |
| XLPE | Cross-Linked Poly-Etylene |
| RMU | Ring Main Unit |

# List of Figures

# List of Tables

<div style="text-align: right">

# 1

</div>

<div style="text-align: right">

# Introduction

</div>

## 1.1. General background

In 2015 The Paris Agreement was signed. It was adopted by 196 countries at the 21st Conference Of Parties (COP21) and entered into force in late 2016. The goal of this agreement was to limit global warming to a maximum of 2 °C by reducing greenhouse gas emission, compared to pre-industrial levels. [1]. To attain this objective, the 195 signatory countries of the agreement are working towards an annual reduction in global greenhouse gas emissions, with the ultimate aim of achieving a climate-neutral world by the middle of the century.

Greenhouse gasses are emitted when fossil fuels are burned in generators, which support the energy need of society. An alternative to this is using renewable energy sources, such as solar and wind power. Stedin and other Distribution Grid Operators (DSOs) will need an added level of flexibility in order to handle the volatility of renewable energy generation in their networkds. This flexibility can be achieved with, for example, the use of storage systems. This is an alternative to the standard option for DSOs, which is traditional reinforcement of the network.

Batteries are of particular interest for distribution system flexibility at the moment. Energy system flexibility is the ability to adjust supply and demand to achieve the matching of supply and demand. After Tennet announced future congestion in Limburg and Noord-Brabant [2], the amount of grid-tied battery connection applications quadrupled with in total 10 times the normal capacity. This is a problem because currently the battery owners are not obligated to contribute to reducing congestion in the network and simply prioritize profit. This could possibly result in the batteries creating more congestion. Legally DSOs are not allowed to be selective in their granting permission of access to their systems of certain battery owners. This means that it will be valuable to look into how these non cooperative batteries are able to be connected to the grid in such a way, that they relieve congestion instead of causing or worsening it [3].

## 1.2. State of the art

Many papers look into the optimal location and size for batteries in networks that do congestion relief. These are usually pertaining congestion relief batteries such as reviewed in [4], [5] and [6]. Batteries that provide the energy arbitrage service are also researched, but the main goal of that research is on how to maximize profit based on location in the grid [7]. There is yet to be a direct comparison between the congestion relief batteries, energy arbitrage batteries and traditional reinforcement with their effect on congestion. The comparison between the congestion relief and energy arbitrage batteries and traditional reinforcement will be researched in this paper.

The research gap that this paper tries to fill is, how useful an energy arbitrage battery is at relieving congestion in a network. It answers this by using an optimally placed energy arbitrage battery in a case study where in congestion occurs. It is possible that batteries alone will not be enough so the remaining

congestion can be taken care of by load curtailment.

## 1.3. Research questions

With the use of Powerfactory and Python a simulation is created. With this, insight into the effectiveness of batteries in fixing congestion is found. The results for combating congestion with cooperative and non-cooperative batteries will be compared to traditional grid reinforcement. The grid that is modeled in Powerfactory is a Medium Voltage (MV) network in the North of Rotterdam. The input data for this is provided by Stedin.

The objective of this thesis is to answer the following research questions:

1. How can a strategically placed battery that uses energy arbitrage be used to relief congestion?
2. What is the most effective location to add a battery in order to relieve congestion?
3. How do the most preferred location for the grid operator and the battery owner differ?
4. How does battery storage compare to reinforcement of the grid when it comes to adding flexibility to the grid?
5. How much better is a congestion relief service providing battery at relieving congestion compared to the battery that uses energy arbitrage?
6. To what extent will load curtailment be needed, when batteries are introduced to the system instead of reinforcing the grid?

## 1.4. Structure of the thesis

The remainder of this report is structured as follows. Chapter 2 will start with introducing methods of network reinforcement and ends with introducing the case study that is used for this thesis. Chapter 3 explores the optimal location and size of energy arbitrage batteries for mitigating network congestion in the case study. It will start with describing the methods and steps that are used in order to create a forecasted price signal and it ends with the creation of the algorithm that is tasked with finding the optimal location and size of the energy arbitrage battery. Then in Chapter 4 the congestion relief battery is introduced. In this chapter the process of altering an existing Powerfactory model into a model that fits the requirements of this thesis is described. The congestion relief capabilities of these three options will be compared with each other in Chapter 5. Finally in Chapter 6 a comprehensive conclusion is drawn. The research questions are summarized and recommendations for future research are provided.

# 2

# Reinforcement

This chapter describes the traditional reinforcement of the grid. First it will be explained what reinforcement entails and what kind of methods are possible to be used in Section 2.1. After that the different cable types that could be used as replacements, are described in Section 2.2. Next the pricing method of the reinforcement will be described in Section 2.3. Lastly the method of determining which cables of the case study will need to be reinforced shall be discussed in Section 2.4.

## 2.1. Tradition Reinforcements

Traditional grid reinforcement refers to the process of upgrading or expanding the existing electrical grid infrastructure to accommodate increased demand, improve reliability, and ensure stable electricity supply. It involves various measures and investments aimed at enhancing the capacity, efficiency, and resilience of the grid. The goal of these improvements is to increase the operational window wherein the grid is able to operate within its limits.

### 2.1.1. Grid limits

Distribution grids, despite operating at lower voltage levels compared to transmission grids, also have operational limits that need to be considered. These limits arise due to various factors and constraints within the distribution system. The operational limits that occur in distribution grids include:

- Voltage Limits: Distribution grids have upper and lower voltage limits that need to be maintained to ensure reliable and safe operation. Exceeding these voltage limits can result in equipment damage, decreased power quality, and potential hazards to connected devices.
- Thermal Limits: Distribution grids have thermal limits on conductors, transformers, and other equipment. These limits define the maximum current-carrying capacity or load that equipment can sustain without overheating. Exceeding these limits can lead to equipment failure, increased losses, and potential outages.
- Power Quality Limits: Power quality parameters such as voltage fluctuations, harmonics, and voltage imbalance have limits defined by industry standards and regulations. Excessive variations in voltage or the presence of harmonics can affect the performance of sensitive electronic equipment, cause malfunctions and result in data loss or operational issues for customers.
- Protection Coordination: Distribution grids employ protective devices such as fuses, circuit breakers, and relays to detect and isolate faults. These devices need to be coordinated to ensure that only the faulty portion of the grid is isolated, while minimizing the impact on the rest of the system. Proper coordination of protection devices helps maintain the reliability and availability of power supply in the distribution grid.

The DSO needs to maintain all these limits in order to ensure reliable operation of the grid and its connected costumers.

Voltage variation limits
In the MV networks of Stedin there is a limit to how much the voltage may vary between two points of a MV network. These limits are visually shown in Figure 2.1.
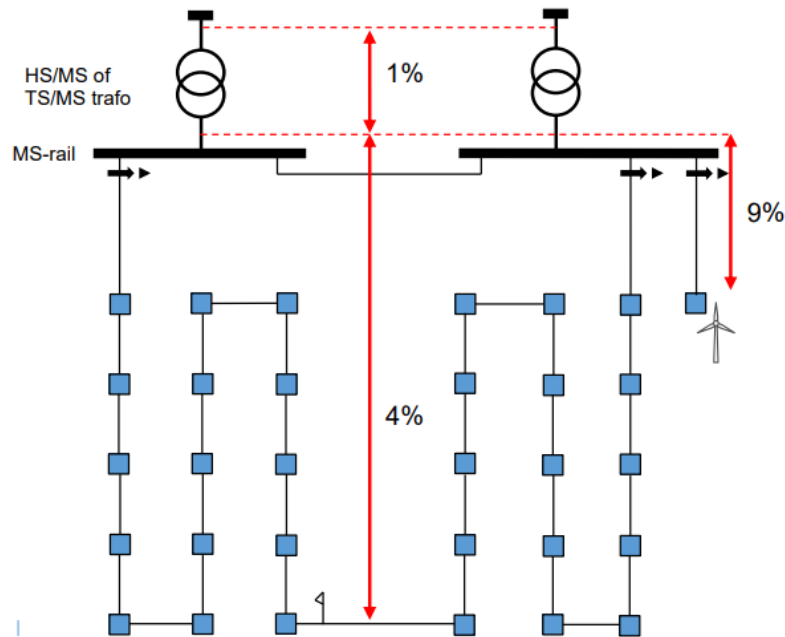


**Figure 2.1:** Allowed voltage swing inside of the MV network [8]

.

The figure shows that the maximum allowed voltage variation for the HV/MV transformers is 1%. For the total group of loads the maximum allowed voltage variation is 4%. Lastly for clients that are directly connected to the transformer station, the maximum allowed variation during normal operation is 9%.

## 2.1.2. Traditional reinforcement methods

In order to ensure the continued operational efficiency of distribution grids amidst anticipated future increases in demand, a range of traditional grid reinforcement methods are available. The traditional grid reinforcement methods for a medium voltage distribution grid:

- Distribution Line Upgrades: Increasing the capacity of distribution lines by upgrading conductors with higher ampacity ratings. This involves replacing existing lines with larger gauge conductors or utilizing compact conductors that can carry more current. This also lowers voltage deviations due to the lower
- Transformer Upgrades: Upgrading distribution transformers to higher capacity units to accommodate increased load demand. This may involve replacing older transformers with more efficient and higher-rated transformers or adding additional transformers to existing substations.
- Capacitor Banks: Installing capacitor banks at strategic locations in the distribution network to improve power factor and voltage regulation. Capacitor banks help reduce line losses, improve voltage stability, and increase the overall capacity of the grid.

Stedin currently looks mainly into the distribution line and transformer upgrades. Capacitor Banks are not used by Stedin, because of the lack of overhead lines in their networks. Overhead lines have a higher amount of reactance compared to underground cables. Capacitor banks regulate voltage by providing reactive power, which interact with the reactance in the network, to counteract voltage drops. Due to the low reactance of underground cables the effectiveness of the capacitor bank is low.

The problem with a voltage variation that is too large is that the promised voltage level for the end user will be affected. In order to fix this, Stedin is able to change the voltage step of the MV/LV

transformers in such a manner, that the resulting voltage at the Low Voltage (LV) side has the required level. Or if the problem is occurring at a few loads in series, a step transformer could be placed in front of the loads at the MV level, in order to keep the voltage at the required level for the loads. At Stedin there are also talks about looking into how much reinforcement investment could be deferred by upgrading the protection infrastructure and protection scheme instead. This would be paired with the closing of the down the line circuit breakers, such as the open circuit breaker shown in Figure 2.1. This is called network reconfiguration: Optimizing the layout and configuration of distribution networks to improve reliability and load balancing. This will change the MV networks of Stedin into either into ring or meshed networks instead of radial networks. This will lead to a more evenly distributed load over the power lines that are closer to the external grids, which would lower the congestion on heavily encumbered power lines. Whether the part network is operated in a radial, meshed or ring layout has influence on the protection scheme that is needed to isolate faults in case they occur.

## 2.2. Cable types

Stedin currently utilizes two types of cables, namely Cross-Linked Polyethylene (XLPE) and Paper-Insulated Lead-Covered (PILC) cables, within its MV networks. The XLPE cables are of a newer generation, while the PILC cables are considered older. In accordance with their age and performance characteristics, the XLPE cables are permitted to operate at full capacity (100%), whereas the GPLK cables are restricted to a maximum capacity of 70% [8].

As per Stedin directives, the replacement of power cables exclusively entails the installation of XLPE cables. This choice is motivated by the fact that PILC cables used lead which is not good for the environment in case damage to the insulation of the cable occurs. Another improvement is the higher current rating exhibited by XLPE cables compared to PILC cables for the same conductor size. Specifically, the conductor diameter for the replacement cables must be either $400mm^2$ or $240mm^2$, as other sizes are incompatible with Ring Main Units (RMUs). Another aspect considered during the cable selection process is whether to employ the trefoil or flat formation of the cables.

Stedin maintains a comprehensive database encompassing various cable types within their inventory. Within this database, the nominal current of each cable is associated with the thermal resistance of the surrounding soil. The thermal resistance, denoting the measure of a material or object's resistance to heat flow, is categorized into three levels in the database: G1 (0.5 [km/W]), G2 (0.75 [km/W]), and G3 (1 [km/W]).

The website cited as [9] provides information on how different types of soil correlate with specific thermal resistances. For instance, wet sand exhibits a thermal resistance of 1, while dry clay has a thermal resistance of 0.75, and wet clay possesses a thermal resistance of 0.5. When the decision is made to replace a particular cable, the geology tool DINO Locket [10] can be utilized to determine the ground type in which the original cable is located. Additionally, the ground water level website of Rotterdam [11] can be consulted to ascertain the cable's year-round moisture conditions.

## 2.3. Pricing

According to Stedin the price per meter for the cables is 350 €/m. This does not change between what type of cable is used, because the price per meter of the cable is only a negligible part of the total costs of placing a cable underground.

## 2.4. Network model data

This section begins by presenting the case study, followed by an explanation of the network analysis method employed by Stedin. Next, the process of acquiring future data is outlined. Finally, the extraction of relevant data from the network is described.

### 2.4.1. Case study

The chosen part network for this thesis is a network in the North of Rotterdam, which operates as a MV network. It operates at 23 kV and consists of 2 traditional generators, 1 wind farm, 2 solar fields, 95 loads, 2 transformers, and 2 external grids. While the network layout is meshed, the practical implementation follows a configuration of 5 radial lines due to multiple circuit breakers being open by

default. This decision is based on the limitations of the outdated protection scheme, which cannot handle bi-directional faults. However, these connections are retained because, following a fault, the downstream loads on the radial network can bypass the faulty line by closing the circuit breaker. The schematic of the network is shown in Figure 2.2.
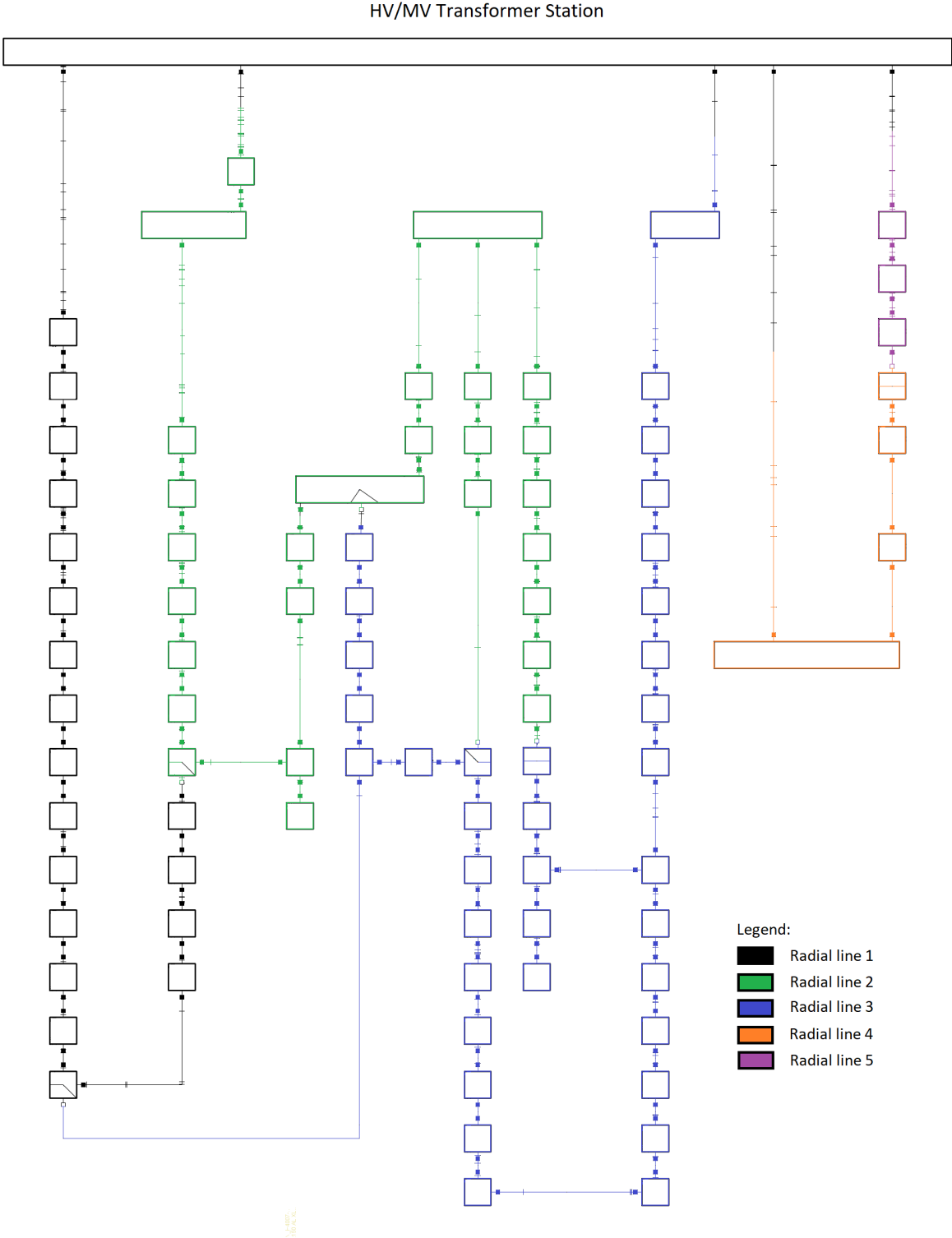


**Figure 2.2:** Case study network.

## 2.4.2. Network analysis application

The power system analysis application that Stedin uses for its MV networks is Powerfactory. PowerFactory is a leading power system analysis software application for use in analyzing generation, transmission, distribution and industrial systems. It covers the full range of functionality from standard features to highly sophisticated and advanced applications including wind power, distributed generation, real-time simulation and performance monitoring for system testing and supervision [12].

Powerfactory functions

Powerfactory provides the Quasi Dynamic Simulation (QDS) feature for conducting medium to long term simulations. This involves performing multiple load flow calculations with user-defined time steps. This tool is especially suitable for planning studies that involve defining long term load and generation profiles, as well as modeling network development with variations and expansion stages. It is a perfect fit for the objectives of this thesis [12]. By analyzing the results obtained from QDS, it becomes possible to determine network congestion.

The QDS function requires a decision on whether to use DC or AC load flow calculations. The determination of the battery's optimal location and voltage level within the grid is important. Taking line losses into consideration is essential for identifying the best grid location for the battery. As a result, AC load flow calculations were chosen because they account for line losses and voltage changes, whereas DC load flow calculations neglect these factors.

Additionally, Powerfactory includes the Sensitivities / Distribution Factors tool. This tool allows users to identify critical points in the network and assess how these points are influenced by changes in system conditions, based on a static voltage stability calculation. It calculates a range of sensitivity factors, including standard distribution factors like Power Transfer Distribution Factors (PTDF) and Outage Transfer Distribution Factor OTDF [12]. The PTDF function provides a matrix that indicates the impact on power flow through all other lines and transformers when 1 MW is injected into a specific node. This feature is particularly valuable when assessing the influence of introducing batteries on grid congestion.

The calculation method of the PTDF will be AC instead of DC, because the AC method takes line losses into account [13]. If line losses are not taken into account, it will be impossible to find the optimal location, because all loads in series will have the same effect on congestion and thus the optimal location finder will not be able to differentiate between the different locations if the locations are connected in series.

## 2.4.3. Future data - SETIAM

There needs to be future data for the QDS to work with. This data is provided by SETIAM. SETIAM stands for Stedin Energy Transition Impact Assessment Model. It was created to assess the effect of the energy transition on the grids of Stedin.

SETIAM utilizes various inputs such as scenarios (in the case of this thesis the KA scenario from Section 3.1.4), grid topology, asset data, measurement data, client requests (for new battery installations), and weather data. By leveraging this data, SETIAM can generate load and generation forecasts up to the year 2050 [14]. These load and generation forecasts serve as crucial inputs for the QDS analysis. Due to complications the only years that were able to be extracted from SETIAM were: 2022,2025,2027,2030, 2035, 2036, 2038, 2040, 2042, 2045, 2050. In the case study the congestion starts to occur from 2036 onwards and thus it is chosen to only look into 2036 and the following years.

# 3

# Energy arbitrage

In this chapter the congestion relief capabilities of energy arbitrage batteries will be explored.

First is Section 3.1. In this section the creation of the market model for the future is described. The market model will take various inputs that are based on research backed predictions and it outputs a price time series signal.In Section 3.2 the design of the energy arbitrage battery will be explained. The depth of simulation, storage technology and the model design will be described and lastly the model will be verified. Finally, Section 3.3 describes how the Power Transfer Distribution Factor (PTDF) and Quasi Dynamic Simulation (QDS) are used in combination with the battery dispatch time series, that was created in Section 3.2, to find the optimal location and size for the energy arbitrage battery.

## 3.1. Energy market modelling

Batteries, like other agents connected to the grid, try to achieve profit while operating. Thus in order to model the behaviour of batteries in an electricity grid, a price signal will be needed. In this chapter the creation of this price signal from 2022 until 2050 will be described.

### 3.1.1. Market options

First the type of energy market that is modelled needs to be determined. Currently there are different kinds of energy markets in The Netherlands. These are the wholesale markets and balancing markets. In this section these markets will be described.

#### The wholesale markets

The wholesale market has two parts, the Day-Ahead Market (DAM) and the intra-day market. For the whole of the Netherlands this is the EPEX SPOT (formerly APX) market [15]. On the DAM participants buy and sell energy on a pan-European auction for the 24 hours of the next day in blocks of 1 hour. At 12:00 the auction is closed and the prices per 1 hour block are determined.

The DAM pricing algorithm is visualized as presented in Figure 3.1a. The merit curves of the demand and supply bits of the auction are put in the same graph. As can be seen in Figure 3.1. For the demand curve the most willing to pay consumers are put in the left of the curve and for the supply curve, the cheapest generation is put to the left of the graph.

This distribution of the consumers and producers results in the most willing to pay consumers and cheap producers bids will be cleared first. The objective of the market is to maximize the total social welfare of the consumers and producers. Social welfare for consumers pertains to how much less the supplied consumers paid for the energy in total, compared to what they were willing to pay. For producers it means how much more is paid for the total generated energy compared to what they offered to generate energy for. The greatest welfare is achieved when the sum of the consumer and generator surpluses are maximized. The price where the two curves meet is the point where the social welfare will be greatest. This is shown in Figure 3.1b.

(a) Market equilibrium                                      (b) Economic welfare
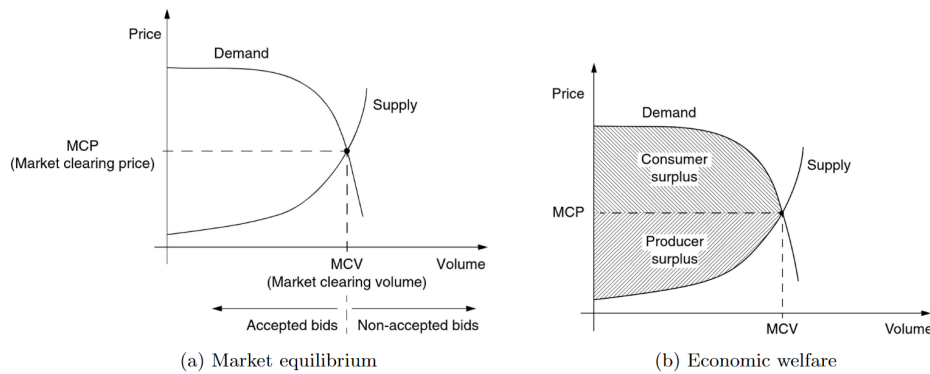
**Figure 3.1:** DAM market clearing price [16]

The prediction that is made by the DAM will inevitably have some prediction error. The discrepancy between the real-time demand and predicted demand is resolved on the intra-day market. On the intra-day market energy can be traded up until 5 minutes before delivery and the time resolution of the delivery is 15 minutes. The goal of the intra-day market is to rectify incorrect predictions that were present on the DAM.

**Congestion management** GOPACS is the congestion management platform of the Dutch DSOs and transmission system operators (TSOs). It uses existing market platforms to find combinations of buy and sell orders that will reduce congestion of the grid. Currently this is used by the ETPA (Energy Trading Platform Amsterdam) [17], which is a Dutch energy exchange that has received a Pan-European intra-day market license [18].

The Balancing Markets
Power fluctuations happen in time periods lower then 15 minutes. This means after the intra-day market correction there will still be some mismatch between generation and demand. This difference is resolved by the balancing markets.
The Balancing markets consist of the FCR market and the FRR market. The FCR market is used for primary control of frequency in the grid. This means that this market is used to catch/stop frequency changes from happening or worsening and the FRR market is used to bring the frequency back to its preferred frequency [19]. In The Netherlands this frequency is 50Hz [20].

## 3.1.2. Role of BESS in the energy market
Battery Energy Storage Systems (BESS) play a significant role in the energy market. The battery systems provide multiple services to the grid. Three of these services are closely tied to the markets that were explained in Section 3.1.1. These services are: Arbitrage, Congestion relief and Ancillary services [21].

Arbitrage
The main goal of energy arbitrage is profit maximization. Energy arbitrage is the practice of buying electricity at low prices and storing it, then selling it back to the grid or consumers at higher prices. It involves taking advantage of price differences over time to generate profits and optimize profit.

Energy arbitrage is best suited for the wholesale electricity market. In the wholesale market, electricity prices fluctuate based on supply and demand dynamics. These dynamic behaviours can be predicted. These price variations create opportunities for energy arbitrage.

In the future renewable energy usage will continue to increase. Consequently, the difficulty of predicting the available generation will be increased. The percentage of the energy that was predicted incorrectly on the DAM and will be cleared on the intra-day market instead will increase as well [22]. This will result in bigger volatility in the price signal and thus a larger profit for BESS. This is supported

by the paper [21] where it was determined that wholesale markets will become viable sources of profits for batteries from 2030 onwards.

Ancillary
Ancillary services refer to additional support services that help maintain the stability, reliability and quality of the electrical grid. The balance market facilitates the ancillary services of frequency control.

Due to the increase in renewable energy production the number of mismatches between supply and demand will increase. If there is more demand than supply, the frequency of the energy will lower and vice versa. Traditionally, frequency control services have been provided by large-scale power plants with the capability to rapidly adjust their generation output.

However, with the increasing integration of renewable energy sources like solar and wind, which are intermittent in nature, alternative solutions are needed to maintain frequency stability. Batteries are beneficial for frequency control services, because of their fast response time[23].

Congestion relief
The congestion relief service aims to alleviate congestion on the electrical grid by strategically managing the flow of electricity. For this service the battery will store excess electricity during periods of low demand and release it during peak demand hours. By shifting the timing of electricity consumption, the battery helps reduce the strain on congested grid infrastructure during peak periods. GOPACS will be able to facilitate this service.

### 3.1.3. Market design
The data that is used for simulating the power flow through the network is given in time steps of 1 hour. This means that the behaviour of the energy arbitrage battery that is to be added needs to have a time resolution of 1 hour as well. The behaviour of the battery is also dependent on the price signal of the market.

If all markets are to be used for the market model, the markets with shorter time steps will need to be translated to determine what their effect will be on larger time scales. The DAM has a time resolution of 1 hour. This means that the modelling of this market will not need to be changed in order to take the simulation time steps of the network into account. As mentioned in Subsection 3.1.1 the intra-day market works with 15 minute time periods. Thus the intra-day market will be cleared 4 times in the time it takes the DAM to be cleared once.

The energy that is traded on the balancing markets is used on a timescale of seconds to minutes [24], which is significantly smaller than the 1 hour time resolution of the power flow data. Modeling the vast complexity and variability of the balancing markets is outside of the scope of this thesis and thus the balancing markets will be neglected. This is equivalent to assuming that the system will have no balancing issues during operation.

This means that only the wholesale markets are to be simulated. As explained in Subsection 3.1.1 the wholesale market consists of 2 markets, the intra-day market and the DAM. In order to simulate the 2 markets as close to reality as possible a two-stage process needs to be implemented. Where first the DAM is cleared and after that the intra-day market is cleared.

intra-day market
There are 3 classes of intra-day market price forecasting. These are: Statistical, machine learning and deep learning [25].

The statistical class uses stationary data where the mean and variance are constant over time. A well known example of the stationary class of a statistical forecasting model is the ARIMA model. The data for this thesis will change over time and thus models of this class cannot be used.
The machine learning (Regression) based models use supervised learning [26], [27] to learn the connection between the intra-day price, the predicted generation, demand and DAM price.

The deep learning class uses deep neural networks [28] in place of the regression model. In order to use these machine learning methods (regression and neural networks) there needs to be a test set of the output (intra-day market clearing price) data, which is used to validate the model. For The Netherlands there is no information about the intra-day energy price and volume per 15 minute period of the past [29]. Thus, the use of machine learning is not possible for intra-day market price of The Netherlands. The countries of which the intra-day energy price was predicted in the earlier cited papers were Turkey and Germany. Turkey's and Germany's past intra-day energy prices are available on the Entsoe Transparency platform [29].

The intra-day market price is influenced by the changing solar and wind power, the generators and congestion that are present in the grid and the layout of the grid. All these variables change between networks, thus the data from other countries is not applicable to The Netherlands. For this reason, it was chosen to only simulate the DAM for this thesis.

This assumes that the DAM predictions are 100 % correct. This is of course not completely realistic because, in reality, it is impossible for the prediction of the DAM to be perfect. This is because of the unpredictability of variable renewable energy generators or unexpected contingencies in generators for example.

### 3.1.4. Energy mix trend
In order to be able to clear the market price the supply and demand curves need to be made for every hour for the years 2022 until 2050.

Scenarios
Netbeheer Nederland has created development scenarios for how The Netherlands is able to become climate neutral by 2050. These scenarios are shown in Figure 3.2. As can be seen in the figure the scenario first splits into 3 scenarios. These are the National drivers (ND), Climate Ambitions (KA) and International Ambitions (IA). The KA scenario is the baseline scenario that the Dutch government is following [30]. The ND and IA are derivations of the KA scenario. The ND scenario looks more into how the Netherlands is able to reach the expected 70% $CO_2$ emissions on its own, by implementing more electrification and using more renewable energies. The IA scenario looks more into the option of more international cooperation and trade in hydrogen and green gas. All three scenarios are made to be able to reach the 70% $CO_2$ emission reduction target by 2035.

It was chosen to use the KA scenario for 2022 until 2035 in this study, because this is most likely the scenario that is implemented in real life because of its governmental support.
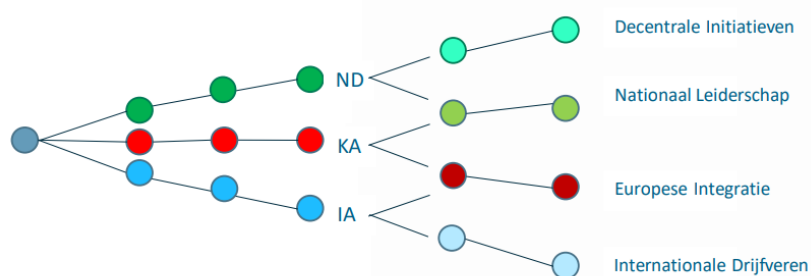


**Figure 3.2:** Overview of scenarios [31]

After 2035 the scenarios are split into 4 scenarios. As can be seen in Figure 3.2 the KA scenario continues into either the National Leadership scenario or the European Integration scenario. The Netherlands has been increasing its cooperation between itself and other EU members when it comes to the energy transition [32], [33] and [34]. For this reason, it was decided to use the European Integration scenario.

Demand

To accurately model the DAM, the demand curve needs to be accurate also. The problem is that the willingness to pay for power of consumers is not available to the public. This is because it could give an unfair advantage for certain agents on the market that could game the system for their own profit. Another option is to create an inflexible demand. The demand is based on an already occurred demand profile which is being scaled, based on the expected demand scaling in the future. By doing this it is important that the solar and wind profiles correspond to this demand profile correctly. As if they are from the same year. The base demand profile is the demand profile of 2018, which is taken from the ENTSO-E Transparency Platform [29]. The reason why 2018 is chosen, because it is the most recent year, where no major world event occurred that influenced the electricity market for example the Covid-19 pandemic and Russo-Ukrainian war. Another reason is that it is the most recent year of the MERRA-2 data set[35], which is used for the profiles of the renewable energies.

The 2018 demand profile was used as the base profile for all the years from 2022 to 2050 and they were scaled based on the scenario data [31]. This can be seen in Figure 3.3
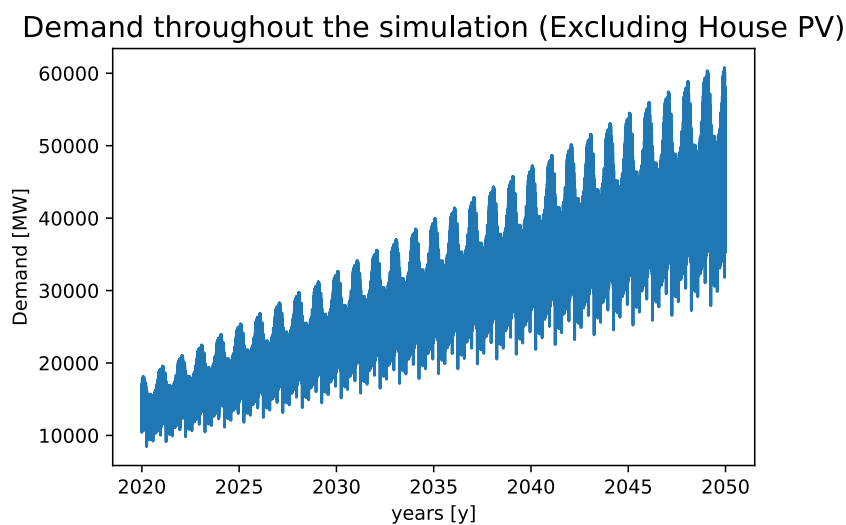


**Figure 3.3:** Base demand throughout the years

**Household PV**   As shown in the future scenario, the amount of rooftop mounted PV panels will increase in the future. These panels will not play a role on the market, but they will influence the total demand that is requested on the market. The solar profile of the household PV is also from 2018 and was sourced from Renewables.ninja [36], which uses the MERRA-2 dataset [35].
Figure 3.4 shows the base demand when household PV is included

**Capacity**   The starting capacity for all the generation types were sourced for the Entsoe Transparency platform [29]. The expected installed capacity of the nuclear power plants is certain, since the government has made concrete plans with the use of legislation for what to do with nuclear energy [37] and coal energy [38] [39]. These expected changes in capacity are shown in Table 3.1.

| Gen Type | 2020 | 2021 | 2024 | 2025 | 2030 | 2030 | 2035 | 2050 |
|----------|------|------|------|------|------|------|------|------|
| **Nuclear** | 486 | 486 | 486 | 486 | 486 | 486 | 3786 | 3786 |
| **Coal** | 4662 | 4012 | 4012 | 2767 | 2767 | 0 | 0 | 0 |

**Table 3.1:** Capacity [MW] changes throughout the years.

Netbeheer Nederland is the association of all electricity and gas network operators in the Netherlands. The energy network operators contribute to the transition to a sustainable energy supply. One

Demand throughout the simulation (Including House PV)
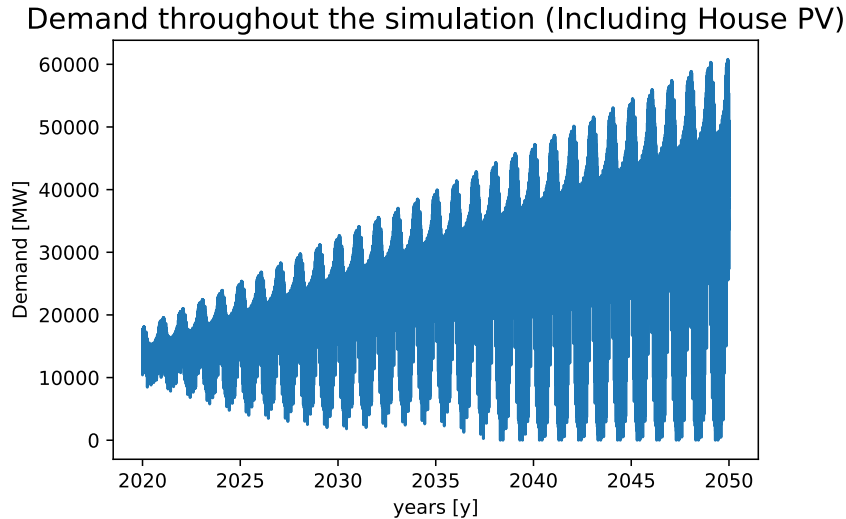


**Figure 3.4:** Base demand including household PV throughout the years

of the key responsibilities of Netbeheer Nederland is to ensure the security and continuity of the energy supply. The association also supports the implementation of innovative technologies and solutions that contribute to the energy transition and the integration of renewable energy sources [40]. Part of this cooperation entails making future predictions of the energy grid and its supply and demand. Netbeheer Nederland has made the Integral Infrastructure-outlook 2030-2050 (II3050), which is the outlook on the future development of the energy system until 2050 for the 3 scenarios explained in Section 3.1.4. As mentioned, the KA scenario was selected and the corresponding values for the capacity per generation type are shown in Table 3.2.

| Gen Type | 2020 | 2025 | 2030 | 2035 | 2040 | 2050 |
|---|---|---|---|---|---|---|
| Gas (aggregated) | 15496 | - | - | - | - | 31800 |
| Biomass | 490 | - | - | - | - | 1100 |
| Solar_field_buildings | 4817 | 28750 | 48750 | 67500 | 82500 | 113750 |
| Solar_households | 2409 | 16250 | 26250 | 31250 | 45000 | 59375 |
| Wind_onshore | 3527 | 7273 | 10000 | 11364 | 16364 | 20909 |
| Wind offshore | 957 | 6364 | 22727 | 29091 | 43636 | 54545 |

**Table 3.2:** Capacity [MW] changes throughout the years.

A graphical representation is shown in Figure 3.5

**Wind and solar profiles**  For the supply side, the wind and solar profiles are sourced from Renewables.ninja [36] for the year 2018. The Wind profile is also included in the MERRA-2 dataset. The magnitude of the profiles will be scaled by the total installed capacity mentioned in Table 3.2.

Supply
For the supply curve, the curve was split in blocks. Each block consists of a grouping of a generation type. Such as Nuclear, Coal, Gas, Biomass, Wind and Solar. For each block the capacity trend and Levelized Cost of Energy (LCOE) are needed as input data for the market model.

**Import element**  Due to the demand being inflexible it is not possible to reduce the demand in case there is not enough supply to meet the demand. This problem does occur in the later years of the
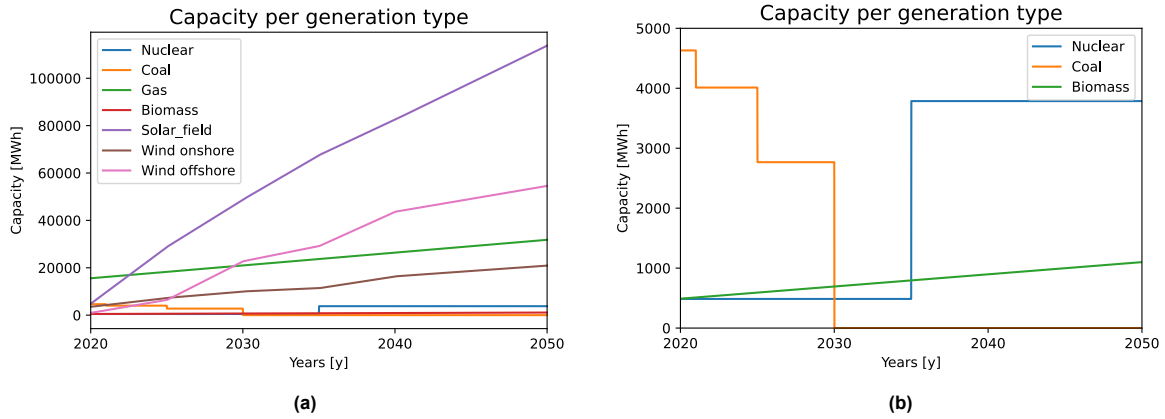
**Figure 3.5:** Trend of the capacity from 2020 until 2050. a) Shows all generation types in the same plot. b) shows a zoomed in view of the graph in order to high light the smaller capacities. Note that the gas graph is the aggregated capacity of all the gas groups.

simulation. In the future this problem can be fixed with the use of batteries and aggregators that participate on the market or by trading in energy with other countries. The battery installations can decide to start discharging when there is too little supply and aggregators can use load curtailment on its own demand in order to help with matching the supply and demand. But including new kinds of elements in the energy market is outside of the scope of this thesis, thus it is decided to only consider the added supply with the use of an import element.

This problem is fixed by adding an import element to the supply. Electricity trading between countries is a common practice in Europe and around the world, and it helps balance supply and demand, optimize energy resources, and improve energy security. The Netherlands is part of the European electricity market and is connected to its neighboring countries through various interconnectors. For example, the Netherlands has interconnections with Belgium, Germany, Denmark, Norway and The United Kingdom. These interconnectors allow electricity to flow between countries, enabling the Netherlands to import or export electricity based on market conditions, demand, and availability of renewable energy sources like wind and solar[41]. Determining the energy mix and expected LCOE for the future of all these connections is outside the scope of this thesis and therefore it is assumed that the energy mix and LCOE prices of the other countries will be the same as The Netherlands. The size of this import element will be 60% of the size of the supply of The Netherlands, because that is the minimum needed for the supply to always meet the demand in The Netherlands.

**Levelized Cost of Energy** LCOE is a metric used to assess the cost of generating electricity over the lifetime of a power plant. The LCOE takes into account all the costs involved in the development, construction, operation, and maintenance of a power generation project, as well as the expected electricity output over its lifetime.

$$LCOE = \frac{I_0 * \sum_{t=1}^{n} \frac{I_t + M_t + F_t}{(1+r)^t}}{\sum_{t=1}^{n} \frac{E_t}{(1+r)^t}} [\text{€}/MWh] \quad (3.1)$$

The meaning of the variables is explained below:

- $I_0$: initial investment expenditures
- $I_t$: Investment expenditures in year t
- $M_t$: Operations and maintenance expenditures in the year t
- $F_t$: Fuel expenditures in the year t
- $E_t$: Electrical energy generated in the year t
- $r$: Weighted average cost of capital (WACC)/ discount rate
- $n$: Expected economic lifetime of the power plant (expressed in years)

The terms $\frac{1}{(1+r)^t}$ in the summation is used to take into account the devaluation of currency or interest on loans over the years of operation.

If a generator sells energy solely at the Levelized Cost of Electricity (LCOE) level, it would precisely recoup its initial investment, assuming no unaccounted events occur in its runtime. In this thesis, the projected LCOEs for different types of generators are utilized as the energy cost for the market. However, employing LCOE as the energy cost poses a challenge, as it would always be lower than the energy cost considered by the generators in their energy bids to the market. Utilizing the LCOE would eliminate the possibility of expecting any profit, as it would only allow breaking even on their investments. Consequently, the actual energy costs used for energy bids by the generators will exceed the LCOE. This will not have an effect on the energy mix of the model, assuming that all generators aim for the same profit margin.
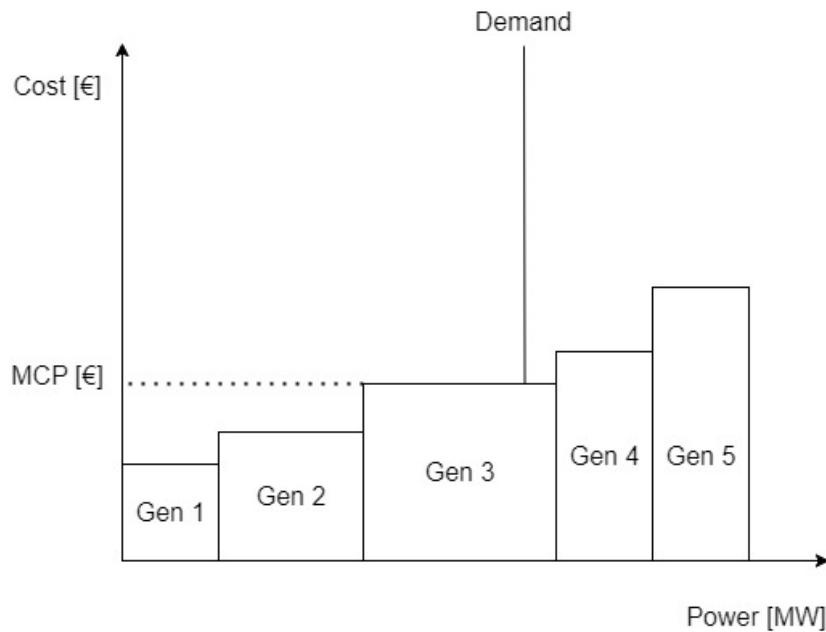


**Figure 3.6:** Day-ahead market

The precise energy prices or price bids per generator are not publicly known. If such information is disclosed, competitors could manipulate the system by setting their prices and capacities in a manner that maximizes their profits at the expense of consumers. For example, generator 3 (Gen 3) in Figure 3.6 could slightly reduce the capacity of its bid, resulting in an increase in the market clearing price or energy price to match that of Generator 4 (Gen 4). As a result, the profits of Generator 3 would be enhanced, but the energy price that consumers must pay would also rise.

The LCOE and energy bid price of a given generator, although not identical, are expected to be similar. Moreover, in the market context, the underlying objective is to employ arbitrage batteries to determine the optimal moments for discharging or charging based on fluctuations in price. This determination is predicated on identifying periods of low and high prices, rather than relying on precise price values. Therefore, the focus lies on price differentials rather than exact prices. Because of this it was decided that LCOE is a realistic approximation of the energy bid prices.
    Table 3.3 shows the trend of the LCOE values of all the generator types from 2020 until 2050. It is important to note that precise data regarding the intermediate time periods between the specified data points is unavailable. For this reason, the price in between the data points is assumed to be linear. Nuclear energy is the exception to this. The Netherlands is beginning on the construction of two new nuclear generators and the current nuclear power plant in Borssele will be refurbished in 2035 [37]. The new and refurbished nuclear power plants will have more efficient power generation. This means that they will have a lower fuel cost as mentioned in the LCOE equation 3.1, which will result in

| Gen Type | 2020 | 2030 | 2040 | 2050 | Reference |
|---|---|---|---|---|---|
| **Nuclear** | 80 | - | - | 80 | [42] |
| **Coal** | 80 | - | - | 65.55 | [43] |
| **Gas** | 50,60,70,80,90,100 | - | - | 50,60,70,80,90,100 | [44] |
| **Biomass** | 107 | - | - | 81 | [42] |
| **Solar** | 70 | - | - | 24 | [45] |
| **Wind onshore** | 59 | - | - | 35 | [46] |
| **Wind offshore** | 84 | 55 | 45 | 40 | [46] |

**Table 3.3:** LCOE [€/MWh] changes throughout the years.

a lower LCOE. The new generators are to be put into action around the same time. This causes the instantaneous drop at 2035.

A graphical representation of the LCOE trend is shown in Figure 3.7.
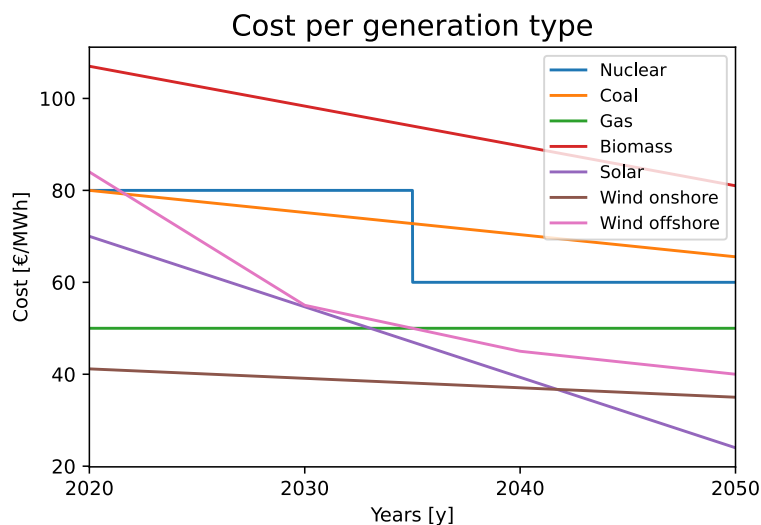


**Figure 3.7:** Trend of the LCOE from 2020 until 2050. Note that of the 6 price levels of the gas generation type only the lowest price (50 €/MWh) was plotted in order to keep the graph clear.

The capacity of the gas generation type was percentage wise large. This caused the price signal to not be volatile. With the price signal staying at the gas price level for multiple years. This is illustrated by Figure 3.8a. It shows that gas power will be the main source of non variable energy and thus will be the generation type that determines the price.

A solution to this is dividing the price signal of the gas generation type into multiple parts. The price range of the gas groups are as shown in Table 3.3 and are based on the data sourced from the International Energy Agency - Levelized Cost of Electricity Calculator [44]. With this method the price will become more volatile, because the demand will move between multiple price levels as can be seen in Figure 3.8.

## 3.1.5. Energy market optimization model
In order to determine the market clearing price (MCP) the market needed to be modelled.

optimization solver
For this model there needs to be a solver in order to clear this market model. The objective function that the solver needs to solve is shown in Equation 3.2 and the constraints are shown below it. The
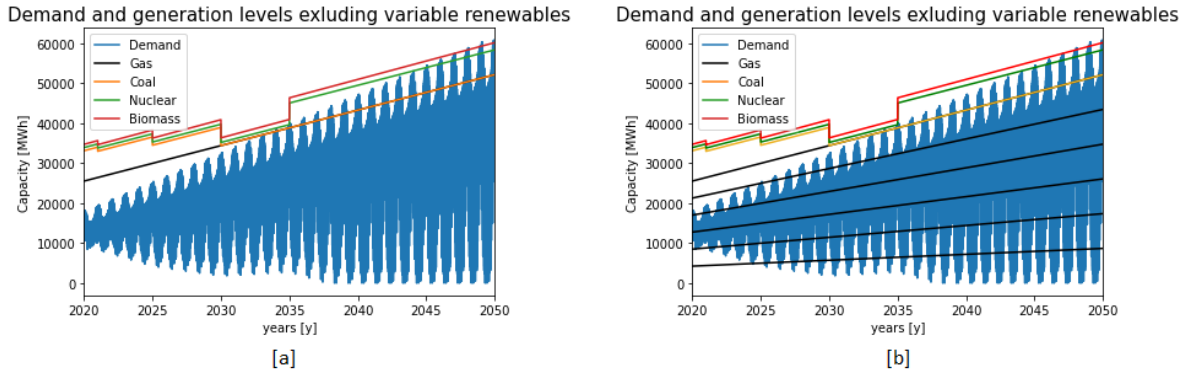
**Figure 3.8:** a) Non variable renewable price levels with only 1 gas group, b) nonvariable renewable price levels with 6 gas groups

objective function and the constraints are all linear. This means it will be possible to use linear programming (LP). There are multiple possible solvers that could be used for LP, such as Optimization Toolbox (MATLAB), Gurobi and CPLEX. The optimization problem will have multiple periods over which the objective function and its constraints will need to be solved. Optimization Toolbox (MATLAB) does not facilitate multi-period optimization problems well, because every single period of every constraint needs to be put inside of a matrix by hand. While in Gurobi and CPLEX all the periods of a single constraint are able to be formulated in one line. While both Gurobi and CPLEX have similar performance and features, there are some differences between them. In general, Gurobi is known to be faster and more efficient than CPLEX, particularly for large-scale optimization problems. Gurobi also has more advanced features for parallel computing and optimization modeling. For this reason, Gurobi was used for this thesis. This solver is capable of calculating LP and Mixed Integer Linear Programming (MILP) models at a fast speed, multiple periods are easy to implement and it is free for university students [47].

## Model Design

The model that clears the DAM price for a single period (1 hour) will be a LP model. The objective of the optimization is the maximization of social welfare as shown below.

$$Max \quad SW = \sum_{j=1}^{N_D} \lambda_{Dj} * P_{Dj} - \sum_{i=1}^{N_G} \lambda_{Gi} * P_{Gi} \tag{3.2}$$

As explained in Section 3.1.1 the demand and supply curves are needed for this.
This objective function is subjected to the following constraints:

$$0 \leq P_{Dj} \leq P_{Dj}^{max} \qquad \forall j \tag{3.3}$$

$$0 \leq P_{Gi} \leq P_{Gi}^{max} \qquad \forall i \tag{3.4}$$

$$\sum_{j=1}^{N_D} P_{Dj} = \sum_{i=1}^{N_G} P_{Gi} \tag{3.5}$$

Note that the congestion constraints for the network are ignored, because the DAM does not take congestion into account when clearing the market [48].

As explained in Section 3.1.4 the demand that is used for this thesis is an inflexible demand, which means that the objective function will become:

$$Max \quad SW = \sum_{i=1}^{N_G} \lambda_{Gi} * P_{Gi} \tag{3.6}$$

The constraint shown in Equation 3.3 will be removed because the demand is not variable anymore. The equality constraint shown in Equation 3.5 will become:

$$P_D = \sum_{i=1}^{N_G} P_{Gi} \tag{3.7}$$

The meaning of the variables is explained below:

- SW : the single-period social welfare (objective function),
- $P_D$ : The inflexible power (constant, given),
- $P_{Dj}$ : the power bid by demand j (optimization variable),
- $P_{Gi}$ : the power offered by generating unit i (optimization variable),
- $P_{Dj}^{max}$ : the MW size bid by demand j (constant, given),
- $P_{Gi}^{max}$ : the MW size offered by generating unit i (constant, given),
- $\lambda_{Dj}$ : the price ($/MWh) bid by demand j (constant, given),
- $\lambda_{Gi}$ : the price ($/MWh) offered by generating unit i (constant, given),
- $N_D$ : the number of demands,
- $N_G$ : the number of generating units.

The price signal per hour was determined by determining what the price of the most expensive dispatched generation type was per hour.

### 3.1.6. Verification

In order to verify if the market model operates correctly, Figure 3.9 was created. The selected date for analysis was March 11th, 2035. This particular day was chosen to demonstrate the impact of reduced energy prices resulting from renewable sources while highlighting the ongoing necessity of traditional generation methods. The LCOE of the dispatch generator groups are shown in Table 3.4.

| Generator type | LCOE [€/MWh] |
|----------------|--------------|
| Onshore wind | 38 |
| Solar | 47.5 |
| Offshore wind | 49.5 |
| Gas 1 | 50 |
| Gas 2 | 60 |
| Nuclear | 60 |
| Gas3 | 70 |

**Table 3.4:** LCOE of dispatched generator groups on March 11th 2035.

In Figure 3.9a it can be seen that the generation groups are dispatched in order of lower price to higher price. It can also be seen that when another generation group becomes the new highest prices dispatched generator group, the price signal in Figure 3.9b changes accordingly to the prices set in Table 3.4.

It is also interesting to note that, because of the large amount of wind energy at the start of the day, the price is kept low at the start of the day compared to the evening.
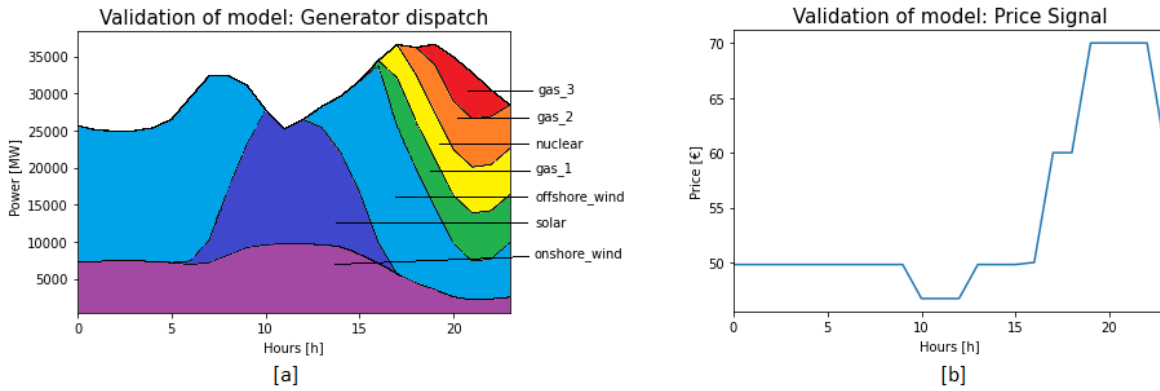
**Figure 3.9:** a) Dispatched capacity per generation type, b) Price signal. Both graphs where made with the data for 11th of March 2035

## 3.2. Energy arbitrage battery model

As explained in Section 3.1.2, the goal of the energy arbitrage is to maximize the profit of the battery. In this section the energy arbitrage battery model is designed. The model has the price signal of the market as an input and outputs the dispatch time series signals of the battery.

### 3.2.1. Depth of simulation

When modelling a battery the first step is to determine what level of depth the model requires. These models can be categorized into three levels based on the degree of physical insight they offer:

- White box model: These models go to the deepest depth. Electrochemical modeling provides a comprehensive description of battery chemistry, ensuring precise representation. These models heavily rely on the electrochemical reactions occurring within the electrodes and electrolyte. By utilizing a set of non-linear differential equations [49], they effectively capture the diverse chemical reactions taking place inside the battery. These methods are accurate but also computational intensive.

- Grey box model: Circuit oriented models represent batteries using an electrical circuit with discrete components such as resistors, capacitors, and voltage sources. These models can capture some dynamic behavior and are commonly used for system-level simulations. However, circuit oriented models may not accurately capture all the internal electrochemical processes of the battery. This results in a lower accuracy but fast computation of results compared to the white box model [49].

- Black box model: These models are based on experimental data and empirical relationships. They typically involve simple equations or look-up tables to estimate the battery behavior. Empirical models are relatively easy to implement but may lack accuracy and may not capture the underlying physics of the battery. Mathematical modelling is primarily used to depict system-level behaviour [49].

Due to the large time frame (30 years with a time resolution of 1 hour is 30 * 8760 = 262800 hours) that is simulated for this thesis it was chosen to use a mathematical model/ black box model depth for the battery model.

### 3.2.2. Data slicing

The input of the battery model is a price signal time series. The model will determine the discharging and charging times in such a way that it maximizes profit while keeping the constraints of the battery into account. This will be further explained in Section 3.2.4.

It is impossible for the battery model to use the entire price signal as its input, because the arbitrage optimization-problem is NP-hard. An NP-hard optimization problem refers to a class of computational

problems that are known to be challenging to solve efficiently. The term "NP" stands for nondeterministic polynomial time, which represents a set of problems that can be verified in polynomial time [50].
This model will be NP-hard because the optimal charge/discharge decision for a battery relies on its state of charge at consecutive time steps, necessitating a full-time horizon scheduling for obtaining the best solution. However, this leads to an increase in the time complexity of the scheduling of the dispatch of the battery, rendering it an NP-hard problem.

In the context of optimization, an NP-hard problem is one where finding the optimal solution requires examining all possible solutions, which grows exponentially with the problem size. In other words, there is no known algorithm that can solve NP-hard problems in polynomial time. However, once a solution is proposed, its correctness can be verified in polynomial time.

The largest time set that was able to be cleared by the battery model that is described in Section 3.2.4 was 5 weeks. In practice the battery owner will not be able to accurately predict the behaviour of the DAM that far into the future. Through contact with a company in the industry it was found that battery owners schedule their operations based on the predicted data from the DAM of the next day. This means that the energy arbitrage batteries optimize their behaviour, based on one day of the DAM forecast. For this reason the battery input data is sliced in groups of 24 each representing 1 hour.

### 3.2.3. Storage technology
There are multiple energy storage types. These are electrical, electrochemical, thermal, mechanical and hydrogen-related [51]. Of these types, the electrochemical storage systems are used for ancillary systems [52]. Of the electrochemical storage systems, lithium-ion batteries are becoming increasingly cost-competitive. The continued decrease in prices for lithium-ion batteries will make lithium-ion batteries important parts of future grids. For example, [53] predicts that after 2030, lithium-ion batteries will be the most competitive energy storage for: energy arbitrage, power quality, grid investment deferral and congestion management. This claim is reinforced by [54], claiming that batteries that using energy arbitrage next to the balancing services will become profitable on the energy arbitrage market from 2030 onwards.
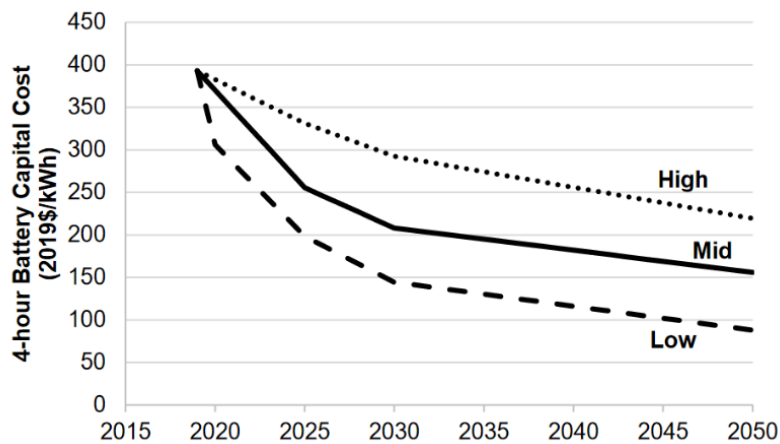


**Figure 3.10:** Trend of 4-hour lithium-ion battery capital costs [55]

Figure 3.10 shows the capital costs trend from 2020 until 2050. As shown the price will decrease from 400 $/kWh to 150 $/kWh. Which is 365.30 and 136.99 €/kWh when converted to Euros with the exchange rate of 2020.

As mentioned in Section 3.2.1, the battery model that is used for this thesis is a mathematical model. Thus, the important properties of the battery need to be included in the model. These properties are: Total capacity, the charging and discharging rate limits and the charging and discharging efficiencies.

### 3.2.4. Energy arbitrage battery model design
There are multiple ways to model a mathematical battery model. One of the important behaviours that the battery needs to be able to model correctly is the fact that discharging and charging does not occur

at the same time.

In order to stop this from occurring, integers could be used. This would make the problem a MILP model. The problem with this is that using integers makes the model much slower. It was mentioned in [56] that the integer constraint could be left out of the model in case the round-trip efficiency property of the battery is included. This however does not always hold true as is explained by two counterexamples [57].

Another option is by using a constraint that is similar but uses a more relaxed constraint as explained in [58]. By relaxing this constraint it is possible that the result will lose some of its accuracy. These two possible models are formulated in Figure 3.11.

| **MODEL** Exact Formulation (**Exact-MILP**) |
| --- |
| $e = E_0 + \eta^c p^c - \dfrac{1}{\eta^d} p^d$ |
| $0 \le p^c \le \overline{P}^c z$ |
| $0 \le p^d \le \overline{P}^d y$ |
| $y + z \le 1$ |
| $\underline{E} \le e \le \overline{E}$ |
| **Variables:** $e, p^c, p^d \in \mathbb{R}_{\ge 0}, z, y \in \{0,1\}$ |

| **MODEL** Relaxed LP formulation (**Relax-LP**) |
| --- |
| $e = E_0 + \eta^c p^c - \dfrac{1}{\eta^d} p^d$ |
| $0 \le p^c \le \overline{P}^c z$ |
| $0 \le p^d \le \overline{P}^d y$ |
| $\underline{E} \le e \le \overline{E}$ |
| $z + y \le 1$ |
| $0 \le z \le 1$ |
| $0 \le y \le 1$ |
| **Variables:** $e, p^c, p^d, z, y \in \mathbb{R}_{\ge 0}$ |

**Figure 3.11:** Constraints of two battery model options, adapted from [58]

After both models were implemented it was found that the relaxed formulation was effective in making sure the battery does not charge and discharge simultaneously. It was also much quicker than the exact formulation model, with the relaxed model taking 3 minutes compared to the 10 minutes of the exact formulation. This is because of the less strict constraint of the relaxed formulation. Therefore it was decided to use the relaxed formulation for this thesis.

The objective function for both the battery models will need to facilitate energy arbitrage:

$$Max \quad Profit = \sum_{t=1}^{T} (Price_t * (P_t^d) - (P_t^c)) \tag{3.8}$$

The variables of the models are explained below:

- $e$ : Energy level of the battery storage at the end of period,
- $E_0$ : Initial energy level at the start of the period,
- $p^c$ : Power that is charged in one period [MWh],
- $p^d$ : Power that is discharged in one period [MWh],
- $z$ and $y$ : z and y represent the binary charging state (z= 1,y= 0), the discharging state (z= 0,y= 1) or idle time (z= 0,y= 0). These variables will become continuous in case of the relaxed LP model,
- $\eta^c$ : charging efficiency,
- $\eta^d$ : discharging efficiency,
- $\overline{P^c}$ : Maximum charging limit [MW],
- $\overline{P^d}$ : Maximum discharging limit [MW].
- $\overline{E}$ : Maximum energy storage capacity [MWh],
- $\underline{E}$ : Minimum energy storage capacity [MWh].

The round-trip efficiency of lithium-ion batteries are around 90% [59]. Assuming the efficiency of charging and discharging to be equal, this would result in $\eta^c$ and $\eta^d$ being equal to 95%. The optimal State Of Charge (SOC) range for a lithium battery is between 20-80% [60]. Thus $\overline{E}$ will be at 80% of

the total capacity of the battery and $\underline{E}$ will be at 20% capacity of the battery.

Next to the operating range of the SOC there is another SOC constraint. This constraint is about what the level of the SOC is at the end of the optimization. Through contact with a company in the industry it was found that there are two options. For the first option the SOC level is set to 50% capacity at the end and start of every day. This coming back to 50% every night is used so ensure the battery is resilient to changes in energy price at the start of the next day. The alternative is having no constraint that dictates the end of day SOC level. Thus, using the last SOC level of the previous day as the initial SOC level of the next day.

For the energy arbitrage battery, the profit maximization has the highest priority. Table 3.5 shows the effect of the SOC setpoint on the profit of a battery with the capacity of 1 MWh. It's important to note that the profits presented in the table are not entirely precise due to their reliance on forecasted LCOE values. However, considering that LCOE provides an approximate future value and the primary aim of the table is to facilitate result comparison rather than showcasing absolute values, it was determined that these values suffice for the comparative analysis.

| SOC setpoint | Profit [€/MWh] |
|---|---|
| 20 (unconstrained) | 119259 |
| 35 | 115207 |
| 50 | 109508 |
| 65 | 101551 |
| 80 | 91732.2 |

**Table 3.5:** Profit per installed MWh for the different SOC setpoints.

The profit is also calculated for when the SOC end point at the end of the day, is unconstrained. In this case the scheduling of the charging and discharging of the battery is identical to, when the SOC has a setpoint constraint, where it always returns to 20% SOC at the end of the day. The reason why the case of a SOC setpoint of 20% and the unconstrained case are equivalent is, because every day the demand in the system peaks between 16:00 until 20:00 o'clock. The average prices signal trend over the day is shown in Figure 3.12. During this time the battery has enough time to completely discharge its contents, after which the price will continue on a downward trend until 24:00 o'clock. Thus, after becoming completely empty, it will need to charge first before it will be able to discharge. This means that the battery will have to charge during high prices and discharge during relatively lower prices which would cost more money than it would gain. Consequently, the battery is empty and it will not charge again, because it would reduce its profit for the day. In the end it will end up empty and thus at 20% SOC.

In Chapter 5 the effect of the 50% SOC setpoint constraint and unconstrained cases on the congestion relief will be shown.

### 3.2.5. Verification

In order to verify the correct operation of the following data needs to be checked: The battery dispatch optimizes profit and SOC limits are held. For this verification the battery with the 50% SOC setpoint was used.

Figure 3.13 shows the demand and the modelled price on March 11th 2035. This the same day that was used in Section 3.1.6.

Figure 3.14 shows the dispatch of the battery and Figure 3.15 shows the corresponding SOC. As can be seen the battery discharges at times of high price and it charges when the price is relatively higher. The goal of the SOC starting and ending at 50% of the total capacity has also verified. The battery also keeps within the SOC limits.
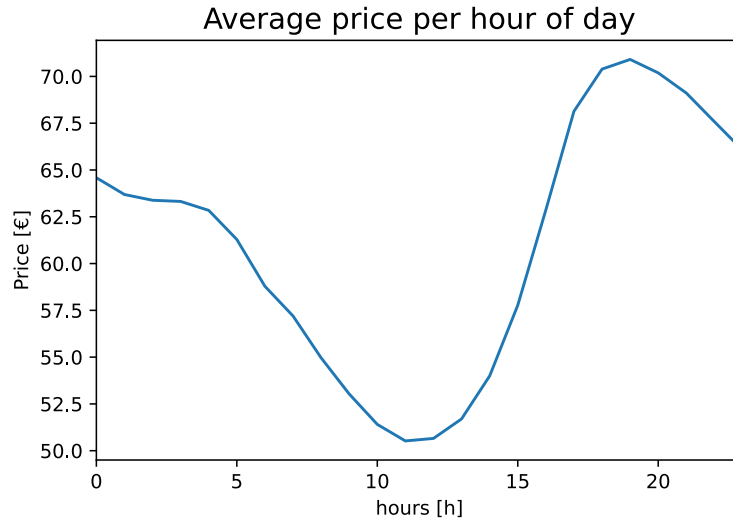
**Figure 3.12:** Average price at different hours of the day of the period 2020 until 2050.
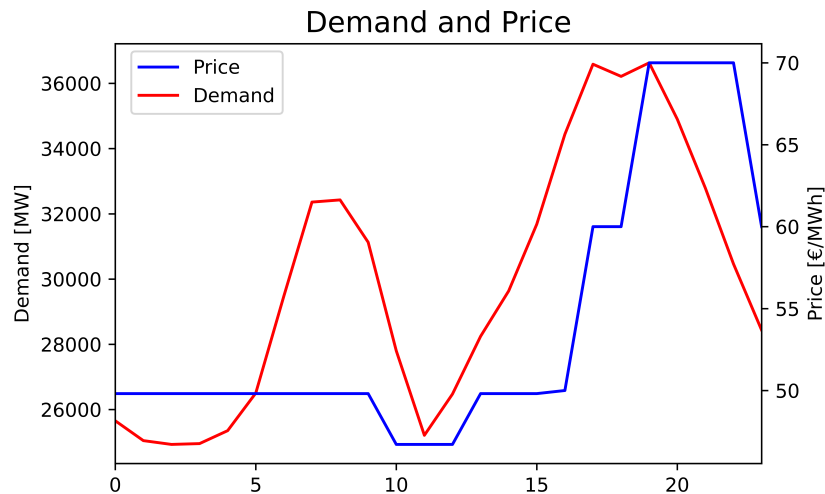


**Figure 3.13:** Demand and Price time series on March 11th 2035

## 3.3. Location and size optimization

In this section the location and size optimization algorithm will be described.

### 3.3.1. location and size optimization algorithm

There are two main groups of methods for sizing and siting of energy storage: mathematical program-
ming and heuristic methods. This thesis deals with a large amount of data and thus the algorithm
should not be computationally demanding. Of the two options, the mathematical programming option
is more computational intensive compared to heuristic methods. Mathematical programming requires
an explicit analytical formulation of the objective function and the constraints. Heuristic methods do
not require explicit mathematical formulations and, for this reason, they are suitable for multi-objective
optimization [59]. The algorithm is tasked with optimizing 2 things: the size and the location of the bat-
tery. Due to the problem being multi-objective and computationally intensive, it was chosen to create
a heuristic algorithm.

For this thesis a greedy search algorithm was selected to find the optimal location and size. The
greedy search algorithm makes use of the problem solving heuristic: choose the locally optimal choice
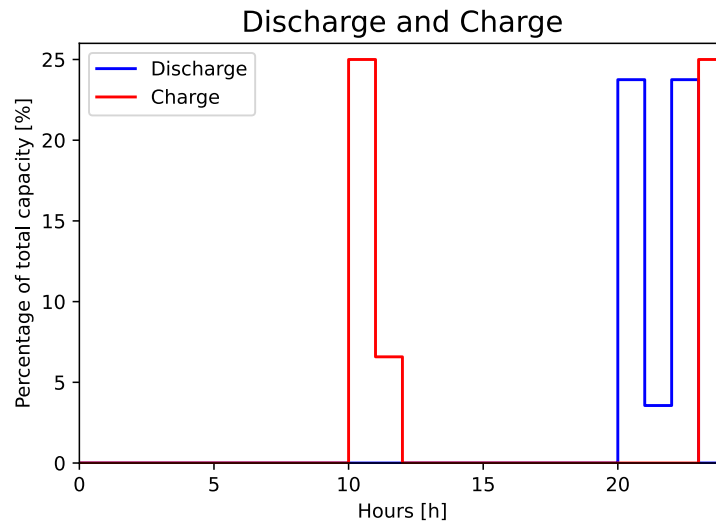
**Figure 3.14:** Battery dispatch on March 11th 2035
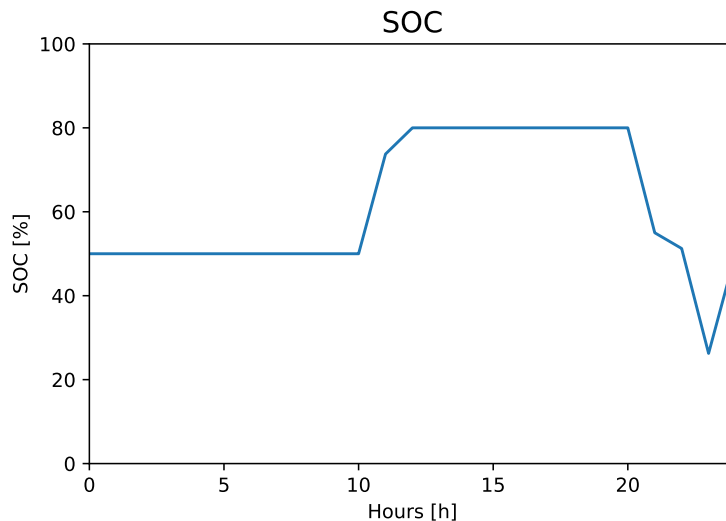


**Figure 3.15:** SOC on March 11th 2035

at each stage. This optimal choice is the option where the highest amount of congestion is reduced. With greedy search algorithms it is possible that its solution is a local optimum.

In Figure 3.16 the greedy solution and the optimal solution are shown. Both start at the top and try to walk the path with the highest value. The path that they take is depicted in grey. The greedy search algorithm only considers the next possible options and chooses the best from the set to walk towards. This leads to a local optimum, because the greedy search algorithm first chooses to go down the right towards the node with value 10 and this causes it to miss out on the node with the 100. The optimal solution is reached by first going to the node with the value of 3 and then towards the node with a value of 100.

With this example it is shown that the greedy search algorithm fails in finding the global optimum if the optimal solution is a path where earlier nodes might have a worse value than later nodes. The only way the greedy search algorithm reaches a global optimum is when the optimal solution path only holds the optimal option for every step.
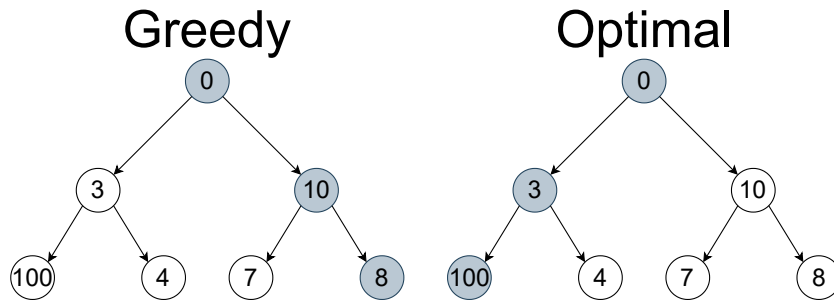
**Figure 3.16:** It is possible that a greedy algorithm fails to maximize the sum of nodes along a path from the top to the bottom, because it lacks the foresight to choose sub optimal solutions in the current iteration that will allow for better solutions later (adapted from [61]).

### Model Flowchart

The flowchart of the whole model, including the greedy search algorithm, is shown in Figure 3.17. On top is the market model. This takes the needed data from online databases and papers to create future time series data for the load demand, capacity and prices of different generation types. This data is converted into a price signal with the use of the market model. Before this data is send to the battery model the data is sliced into slices with the size of 1 day (24 data points for 1 hour each). The energy arbitrage battery model uses this data with the parameter data that was sourced out of papers to create the scheduling of the charging and discharging of the battery in order to maximize profit.

After that, the implemented greedy search algorithm is shown. The goal of the algorithm is to add a battery of the size of $0.05MWh$ iteratively at the location in the grid, where it will cause the most amount of congestion relief.

First the PTDF data of the case study network is loaded in and the load flow without any added batteries (initial load flow) is loaded in. The battery dispatch (discharge and charge) data is combined with the PTDF data and multiplied by the size of the added battery ($0.05MWh$). The created matrix is a 3-dimensional matrix. The first dimension is a list of all the different bus bars in the network, the second is a list of all the power lines and transformers and the third is a time series with the change in power flow in every power line if the battery is added at bus bar x.

By adding the initial load flow to this, all the possible new load flows are determined. Then with the use of the Power limits of the lines data, the new amount of congestion in the system is determined for every possible load flow. Then the load flow with the lowest congestion is chosen. The algorithm will run for 240 iterations. 240 was chosen, because the algorithm was not able to further reduce congestion after 240 iterations. After every iteration the installed battery capacity, its location and total congestion is logged and the next iteration will start. If the congestion level does not improve after an iteration it means there is no longer any congestion that the energy arbitrage is able to improve upon and the battery is placed in the HV/MV transformer station. The charging and discharging that occur there are completely counteracted by the external grid, which acts as a slack and the power lines that are between the HV/MV transformer station and the external grid have enough capacity to not become congested. After all iterations are done the logged data is printed and the simulation is stopped.

### Viability assessment of algorithm

The greedy search algorithm is able to approach the global optimum for the case study that is used for this thesis. This is due to two factors: the topography of the grid as shown in Figure 2.2 and the independence of dispatch scheduling of the energy arbitrage battery.

The power flow consistently moves in the same direction, originating from the external grids and supplying the loads. This is because the network is radial and the generation capacity within the case study network is not sufficient to surpass the local load demand. Consequently, the role of the battery discharge is always focused on relieving congestion, while the battery charging increases the load on
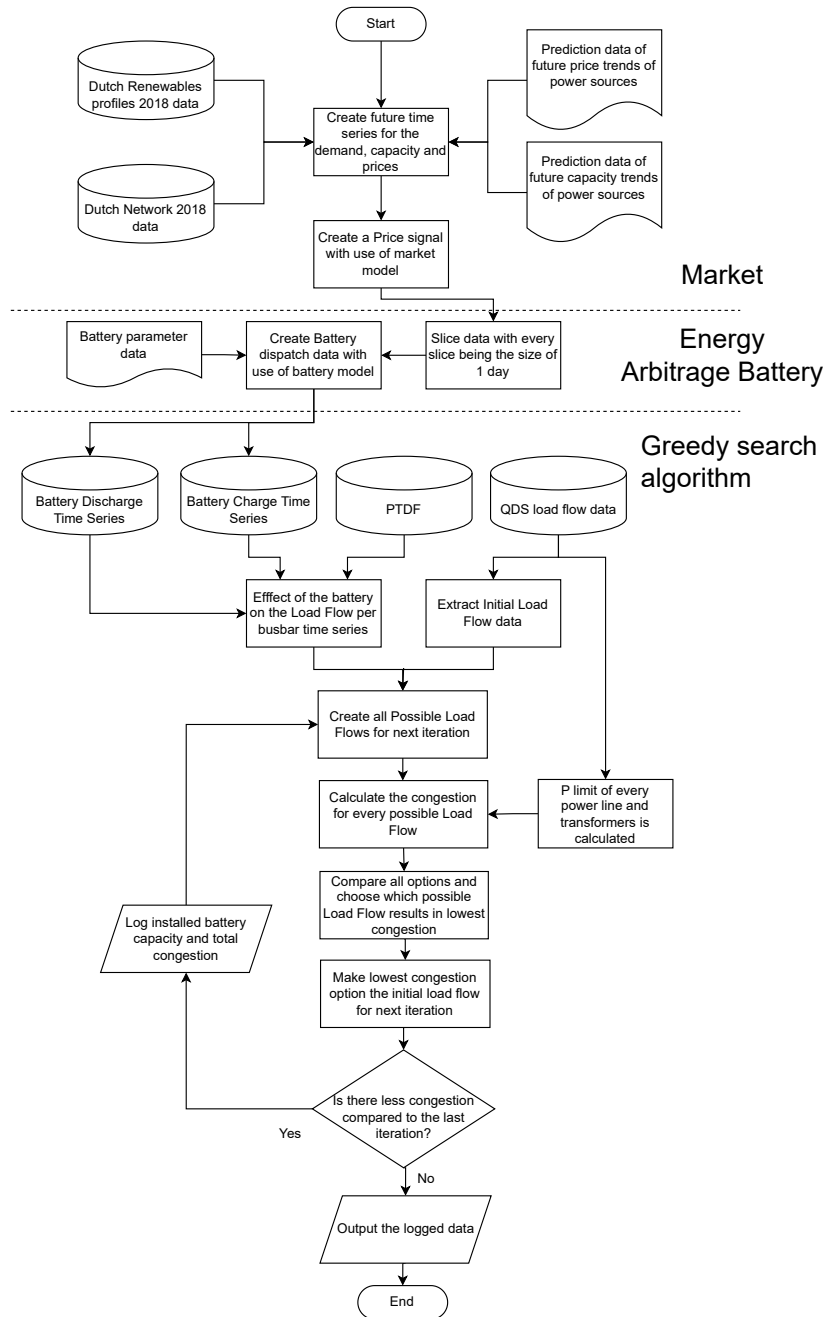
**Figure 3.17:** Flowchart of whole model. On the top is the market flowchart in the middle the battery flowchart model and below the greedy search algorithm flowchart.

the power lines.

The algorithm tries to optimize two things: the location and the size of the battery. For this case study there is only one type of location that is the best location for the battery and that is the deepest part of the radial line. This is because of the losses that occur over the power lines. Equation 6.1 shows a general equation for the power flow through a radial line in case the power always flows from the outside grid towards the radial grid.

$$Power flow = (1 - Fraction_{Line\_loss}) * (Demand_{Radial} - Supply_{Radial}) \tag{3.9}$$

- $Power\,flow$: The amount of power that flows from the outside grid towards the radial line.
- $Fraction_{Line\_loss}$: Fraction of power that is lost while the power is flowing from the external grid towards the radial loads.
- $Demand_{Radial}$: The demand of the loads in the radial line.
- $Supply_{Radial}$: The supply of the generator in the radial line.

The equation shows that the power flow decreases in case of higher line losses and when the supply on the radial line increases. The location with the highest amount of losses is the deepest parts of the radial line, because the power needs to travel the furthest.
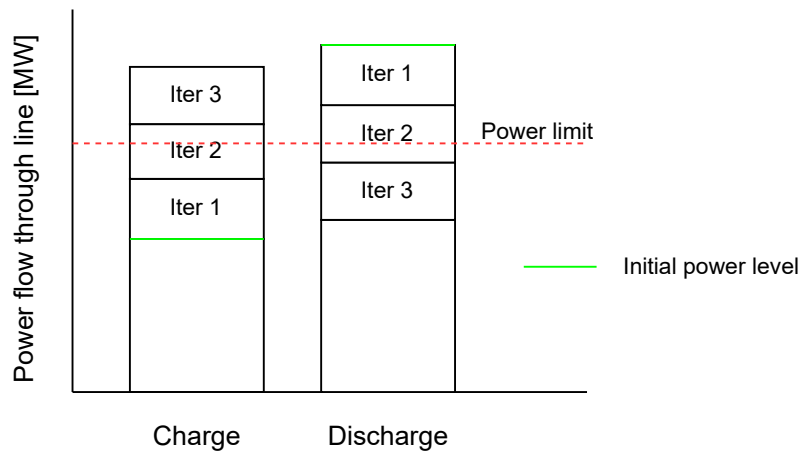


**Figure 3.18:** Effect of greedy search algorithm iterations on congestion (Iter #, stands for iteration number #)

Figure 3.18 shows a simplified version of the effect multiple iteration of adding a battery on the congestion of the network of the case study. To the left the effect of charging of the battery on the congestion is shown and to the right the effect of discharging is shown. As explained earlier the discharging of the battery has a positive effect on congestion, because it reduces the power flow through the power line. As can be seen in the first iteration, the discharging battery reduces congestion and the moment when the battery charges it does not cause congestion. In iteration 2 the charging causes and the discharging relieves congestion. In this cause there is more relief of congestion compared to caused congestion. In Iteration 3 the discharging does not relieve congestion and the charging only causes congestion. In this case the algorithm would put the battery in the HV/MV transformer station and it would not be taken into account for the end results. The scheduling of the discharging and charging of the battery does not change throughout the iterations. The effect of the battery on the power flow also does not change if the battery capacity is placed in the same spot. This means that the algorithm will always approach the optimum solution, because the algorithm will continue to add capacity to the optimum locations until it does not help relieve congestion anymore. The solution will have a $0.05MWh$ margin of error due to the size of the battery capacity that is added to the grid every iteration.

### 3.3.2. Reducing computation time
The algorithm encounters a significant amount of data, resulting in a slow performance (approximately 30 minutes without reducing computational complexity for every year of the simulation). With 6 separate years to look into this simulation, it would take 3 hours to obtain a set of results. This is especially too long if the parameters are changed and the simulation needs to be done again.

The computation time increases as the algorithm incorporates more variables or encounters greater complexity in the model. To mitigate this, it is necessary to streamline the computation process by filtering the data. Specifically, data that is irrelevant to the objectives of this thesis such as data where congestion is unlikely or non-existent, should be excluded. Only data points where the power is either above or slightly below the power limit, indicating the potential for congestion, should be retained. In cases where there is no power dispatched by the energy arbitrage battery, data points where the power

is just below the power limit can also be filtered out. This results in the data set to become smaller.

Another variable that can be filtered is the potential locations for the placement of the battery. If it considers all locations, it will also have to calculate the effect for battery placement for those locations. As the network has radial lines, the changes in load flow that occur in one radial line has no effect on other radial lines. Thus, the locations on radial lines with no occurrence of congestion are also not considered for battery placement. Since there are only 2 of the radial lines with congestion, this leaves only 2 radial lines.
In order to optimize the placement strategy, the algorithm selects positions that are farthest from the external grids within the radial grid structure. As explained in the previous section, this is because the grid is radial and the model takes line losses into account. When the demand is situated further away from the external grid, more power needs to be injected into the radial network by the external grid. By alleviating the load in distant areas, the external grid is required to supply less power to the radial network compared to reducing demand in close proximity to the external grid. This means that only considering nodes located at the end of a radial branch can further reduce computational time while maintaining effective optimization. After filtering the input data and the considered locations, the runtime of the algorithm was reduced to 3 minutes per year of simulation and thus its takes 18 minutes instead of 3 hours to find the exact same set of results.

<div style="text-align: right; font-size: 4em;">4</div>

# Congestion battery

For the congestion battery there is a congestion battery model that is modified in order to meet the requirements for this thesis. First a short background on congestion relief batteries will be given in Section 4.1. In Section 4.2 an example congestion relief battery is described. The way this example congestion relief battery is altered in order to fit the requirements for this thesis is shown in Section 4.3.

## 4.1. Congestion relief background

As mentioned in Section 3.1.2, the battery will store excess electricity during periods of low demand and release it during peak demand hours. By shifting the timing of electricity consumption, the battery helps reduce the strain on congested grid infrastructure during peak periods.

The deployment of congestion relief batteries offers several benefits. First, it enhances grid reliability and stability by alleviating bottlenecks and reducing the risk of voltage instability. Second, it promotes the integration of renewable energy sources by storing excess energy generated during periods of high renewable generation and releasing it when needed, effectively mitigating the intermittency of renewables. Lastly, it enables more efficient utilization of existing grid infrastructure, potentially deferring costly grid expansion or upgrades [62].

## 4.2. Powerfactory example model

In the Powerfactory manual there is an example of a congestion relief battery [63]. It measures the power over a line and tries to reduce the power through the line when it exceeds a pre set level and when the power through the line becomes lower than a certain level, the battery will start to store power.

In Figure 4.1 the control strategy of the generic battery is shown and in Figure 4.1 the related parameters of the model are shown. This battery is easily changed to a congestion relief battery by altering the model.

The battery measures the amount of energy that moves in the opposite direction of the battery, over the power line when the power of the battery is neglected. This is the $P_{line}$ / red line. The $P_{line}$/ green line shows the battery power that moves over a selected line in the direction away from the battery. As can be seen in Figure 4.1 when the red line exceeds $P_{StartStore}$ the battery starts to store energy. The amount that it stores is determined by how far along the value is between $P_{StartStore}$ and $P_{FullStore}$ proportionally to how much the red line exceeds the $P_{StartStore}$ value. The opposite of this happens when the red line goes lower than the $P_{StartFeed}$ value. Figure 4.1 also shows that when the red line exceeds the $P_{FullStore}$ or $P_{FullFeed}$ values, the battery will hit its rated power limit and will cap its power. In this case the battery will not be able to fully lower the congestion.

The flowchart of this battery as described in the Powerfactory manual is shown in Figure 4.2. First the maximum available power for feeding (discharging), $P_{Feed\_limit}$, and storing (charging), $P_{Store\_limit}$, is determined which are based on the available room inside of the battery.
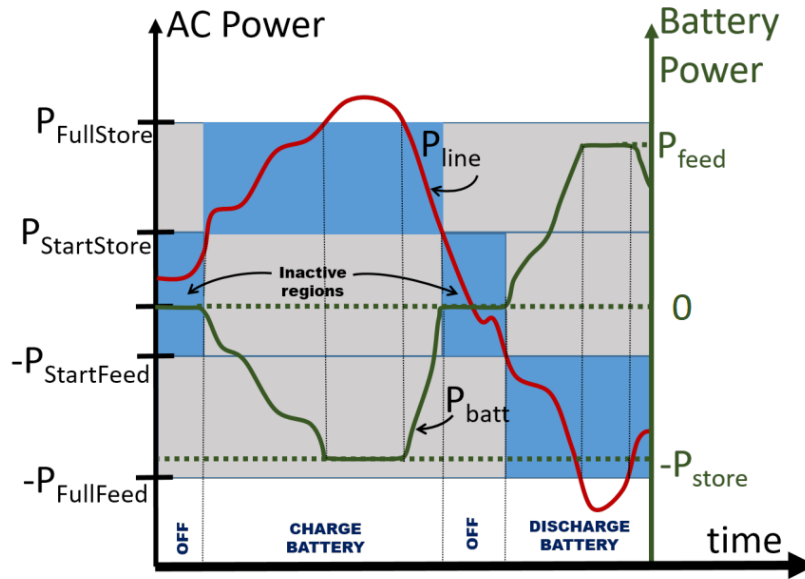
**Figure 4.1:** generic battery control strategy [63].

| state variable | SOC | % | State of charge |
|---|---|---|---|
| parameter | Eini | MWh | Storage Energy Size |
| parameter | SOCini | % | Initial state of charge |
| parameter | SOCmin | % | Minimal state of charge |
| parameter | SOCmax | % | Maximal state of charge |
| parameter | Pstore | MW | Rated charging power |
| parameter | PFullStore | MW | Pmeas where maximum charging is reached |
| parameter | PStartStore | MW | Pmeas where charging starts |
| parameter | Pfeed | MW | Rated discharging power |
| parameter | PStartFeed | MW | Pmeas where discharging starts |
| parameter | PFullFeed | MW | Pmeas where maximum discharging is reached |

**Table 4.1:** Parameters of the congestion battery from the Powerfactory manual [63].

Then the operating region (feeding, storing or inactive) is decided with the use of decision blocks. After which the corresponding $P_{Batt}$ is calculated. Subsequently it is checked if the $P_{Batt}$ exceeds the maximum available power for feeding or storing. The lowest of the two will be set as the new $P_{Batt}$. This way the battery will not exceed the $SOC_{min}$ and $SOCmax$ limits. Finally, the new SOC value is calculated by converting the $P_{Batt}$ value into the amount of SOC change the battery will cause and adding it to the previous SOC value.

The power in the case study network flows only in one direction. This is in the direction towards the congestion battery. In order to lower the maximum amount of congestion it should always be ready to discharge and should fill its battery whenever is possible while not causing congestion. This means it should try to increase the power through the line when there is no congestion up to the congestion amount. Thus, the inactive region from the battery should be removed. Also, the battery model assumes that the battery has 100% efficiency, that there are no line losses and that it is located directly next to the congestion causing line.

## 4.3. Final congestion relief battery
Figure 4.3 shows the flowchart of the altered version of the congestion relief battery. As can be seen the inactive region part of the flowchart is removed. Also instead of using $P_{StartStore}$, $P_{StartFeed}$, $P_{FullFeed}$ and $StartStore$, only $P_{congestion\_limit}$ is used as a coordinate in order to make it more easy to read.
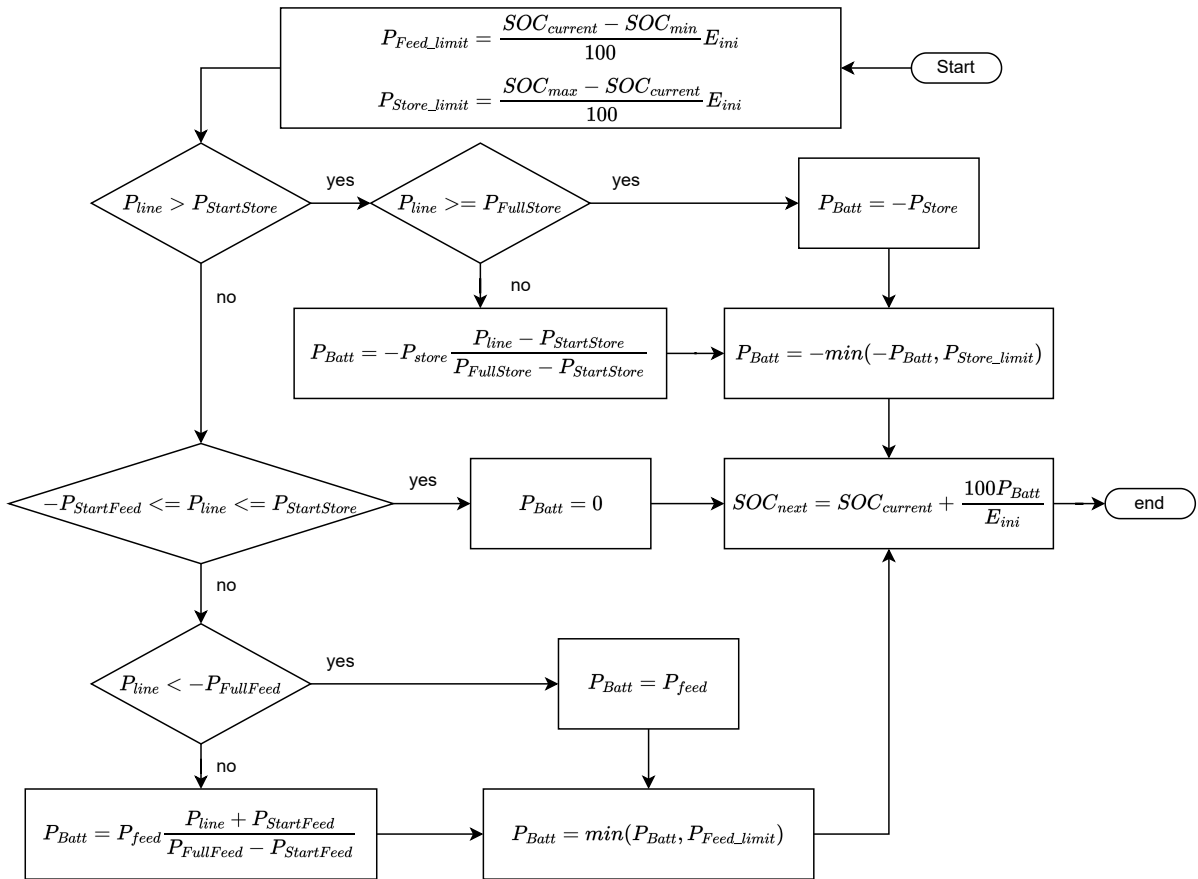
**Figure 4.2:** Flowchart of how $P_{Batt}$ and the SOC value are determined for one time slot by the battery model described in the Powerfactory manual

In addition to that, the direction of the power flow is assumed to go towards the battery, which is in line with the case study. Lastly, the efficiency of the battery and the PTDF value are included. The efficiency is the ability to convert power into stored energy and vice versa.

The battery is sized and located the same as the energy arbitrage battery, while also having the same parameters as the energy arbitrage battery. This way the two services will be able to be compared.

$$P_{Feed\_limit} = \eta_{discharge} \frac{SOC_{current} - SOC_{min}}{100} E_{ini}$$

$$P_{Store\_limit} = \frac{1}{\eta_{charge}} \frac{SOC_{current} - SOC_{min}}{100} E_{ini}$$

Start

$P_{line} < P_{congsetion\_limit}$ — yes → $P_{line} <= P_{congsetion\_limit} - P_{Store} \cdot PTDF$ — yes → $P_{Batt} = -P_{Store}$

no

no

$$P_{Batt} = -P_{store} \frac{P_{congestion\_line} - P_{line}}{P_{Store} \cdot PTDF}$$

$$P_{Batt} = -min(-P_{Batt}, P_{Store\_limit})$$

$$SOC_{next} = SOC_{current} - \frac{100 P_{Batt}}{\eta_{discharge} E_{ini}}$$

end

$P_{line} >= P_{congsetion\_limit} + P_{feed} \cdot PTDF$ — yes → $P_{Batt} = P_{feed}$

no

$$P_{Batt} = P_{feed} \frac{P_{line} - P_{congestion\_limit}}{P_{feed} \cdot PTDF}$$

$$P_{Batt} = min(P_{Batt}, P_{Feed\_limit})$$

$$SOC_{next} = SOC_{current} - \frac{100 \eta_{charge} P_{Batt}}{E_{ini}}$$

**Figure 4.3:** Flowchart of the improved congestion relief batter of how $P_{Batt}$ and the SOC value are determined for one time slot.

# 5

# Results

In this chapter the results of the simulations are explained. First the case study is explained in Section 5.1. Secondly the results for the traditional reinforcement is shown in Section 5.2. Next the results of the energy arbitrage battery cases are shown in Section 5.3 and after that the results for the congestion battery are shown in Section 5.4. Lastly, the research questions will be answered and discussed in Section 6.1.

## 5.1. Case Study

In order to determine the effectiveness of energy arbitrage batteries a case study had to be chosen. The case study had to have its own congestion that was high enough to warrant traditional reinforcement as well. With this the energy arbitrage battery effectiveness in congestion relief will be able to be compared to traditional grid reinforcement.

The location that was chosen was a MV grid in North Rotterdam, a Medium Voltage (MV) network, operating at 23 kV and consisting of various components, including traditional generators, renewable energy sources such as wind farms and solar fields, multiple transformers, external grids, and numerous loads. While the network layout appears meshed, the presence of multiple open circuit breakers in Figure 5.1 indicates a practical configuration of five radial lines. Congestion will start to occur in the network from 2036 onward.

## 5.2. Traditional reinforcement

For the traditional reinforcement only, the lines need to be replaced with new ones. The full QDS needs to be run in order to find the location of the congestion. Normally replacing a power line would cause a change in the load flow, which could cause new congestion in another part of the network. This is not the case for this network, because this network is radial. In total there are 3 lines where congestion occurs, which are shown red in Figure 5.1. As can be seen there is one congested line in Radial line 2 and two in Radial line 3. All three are old PILC cables. Their geographical locations are shown in Figure 5.2. Figure 5.2a being the geographical location of the red congested lines to Radial line 3 in Figure 5.1 and Figure 5.2b is the congested line of Radial line 2. For the other cables there is no reinforcement needed. In Radial line 4 and 5 the congestion peaks at 6% of total capacity and for Radial line 1 it is 30%. The non congested cables in Radial lines 2 and 3 peak at 60% and 65% respectively in 2050.

The lines of Figure 5.2a have a power limit of 7.6 MW and its peak load is 8.355 MW (0.775 MW overshoot). The two congested lines combined are 2.186 km long. With 350 €/m this results in an investment cost of 0.765 million Euros. The other congested cable has a max power limit of 8.142 MW and a peak load of 11.4 MW (3.258 MW overshoot) and is 6.4 km long, which results in an investment cost of 2.24 million Euros. This results in a total of 3.005 million Euros.

By investing in this reinforcement of the grid, the power through the lines will not reach congestion limits in 2050. This means there will be no need for reducing the load with the use of curtailment or other methods. Flexibility will therefore be less needed inside the case study network.
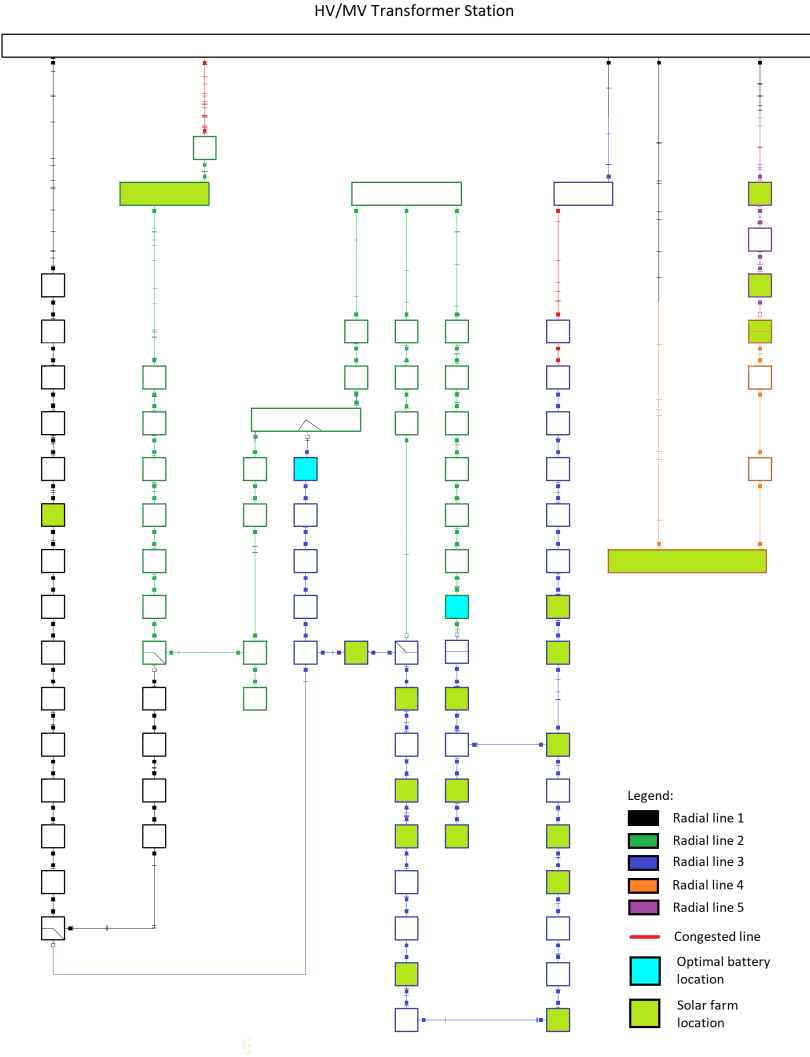
**Figure 5.1:** Case study network
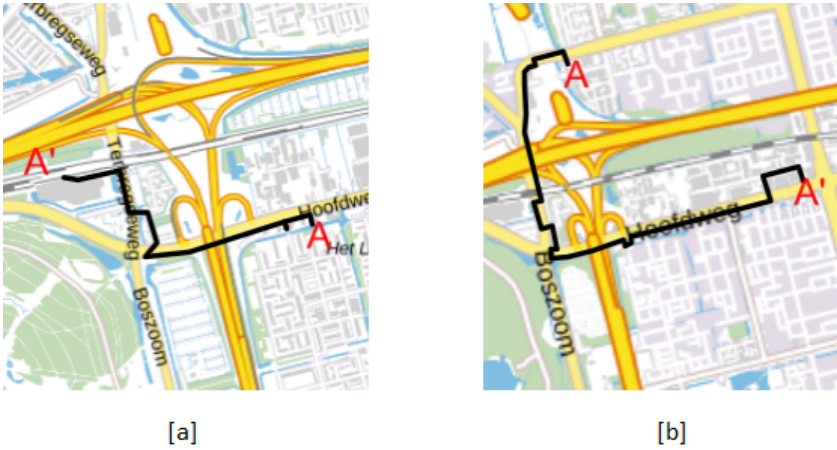


**Figure 5.2:** Geographical representation of congested lines [10].

## 5.2.1. Ground data

The ground in which all the power lines lay is the same. Figure 5.3 shows the ground data profile of the region. The dark blue and orange layers are clay regions and the yellow and light blue are sand

layers. As explained in Chapter 2 it is preferable that the congestion line is put in a clay layer because of its heat diffusing properties. These heat diffusing properties become even better when the wire is submerged in water/wet soil.
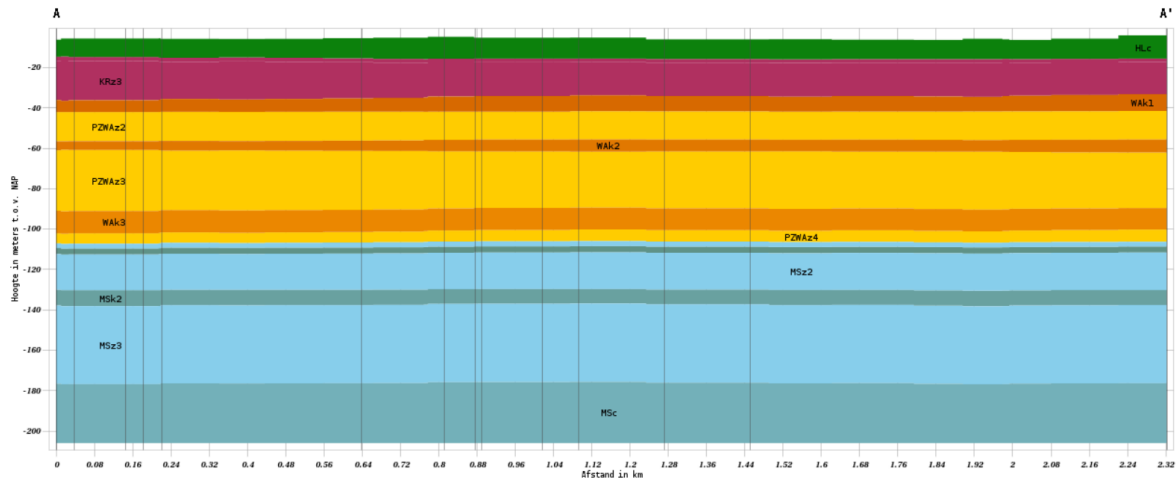


**Figure 5.3:** Ground data profile of the case study region [10].

While the ground type does not change in the region, the ground water level does change. With the data obtained from Geographic Information Rotterdam (GIS) [11] it was found that north of the highway the water level was 1.8 m below the ground minimum and south of the high way the water level never goes under 1.1 m. The locations of the water depth meters in the region are shown in Figure 5.4.
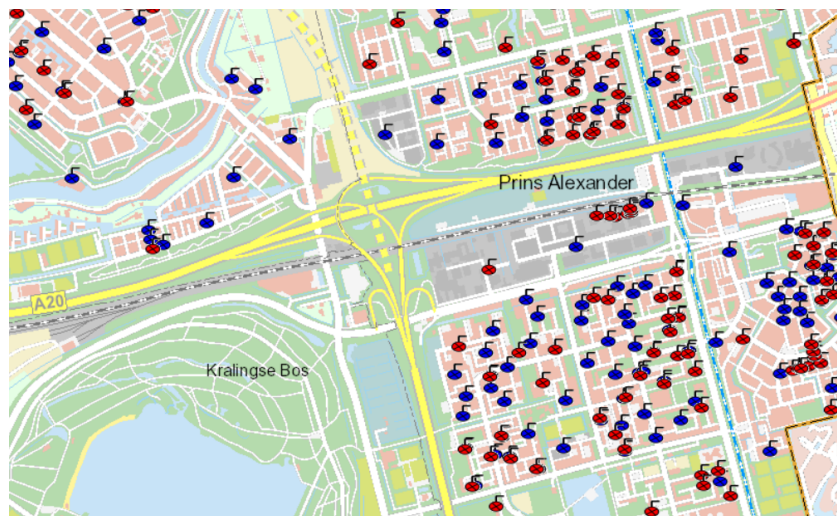


**Figure 5.4:** Location of Water depth meters [11].

Table 5.1 shows that the 3x1*400 AL XLPE 18/30 trefoil will give the highest possible power limit. This can be achieved for both lines by putting the wires in the clay layer at 1.8 meters deep. Since the price of the individual cables does not affect the total price of reinforcing the cables, the 3x1*400 AL XLPE 18/30 trefoil was chosen as best cable to reinforce the network with.

## 5.3. Energy arbitrage battery

The energy arbitrage battery will be applied to two different cases. First the optimally located and sized battery installation will be applied and that will be compared with the case where the optimal size of

| Replacement cable candidate | P limit in wet clay | P_limit in dry clay |
|---|---|---|
| 3x1*240 AL XLPE 18/30 trefoil | 10465 | 8740 |
| 3x1*240 AL XLPE 18/30 flat | 10810 | 8855 |
| 3x1*400 AL XLPE 18/30 trefoil | 13110 | 10810 |
| 3x1*400 AL XLPE 18/30 flat | 12880 | 10465 |

**Table 5.1:** Power limits of candidates for upgrading the congested lines.

the battery of the previous case is distributed evenly over the solar farms inside of the grid. Radial line 1 and 2 have 1 solar farm each, Radial line 3 has 14 solar farms and Radial lines 4 and 5 have 2 solar farms each. The total installed capacity for every case will be the same as the size of the optimal solution of the Optimal Location and Size case. This is in order to compare the effects of the different battery and localization strategies.

### 5.3.1. Case: Optimal Location and Size

In this case the algorithm has decided where to place the battery capacity and also how much. Each step of the algorithm was 0.05 MWh capacity. Thus, the resulting capacities on the locations have a 0.05 MWh margin of error. The results of the optimal location and size case are given for the 50 % and no SOC setpoint constraint cases. As shown in Section 3.2.4, the constraint case will yield a higher profit compared to the 50% SOC setpoint constraint. Table 5.2 shows the results for the unconstrained case and Table 5.3 shows the results of the 50% SOC setpoint constraint. Both tables are structured the same:

- Initial Congestion: This is the congestion in the network without the introduction of a battery.
- New Congestion: This is the congestion after the battery has been placed inside of the network.
- Percentage reduced congestion: This is the percentage of congestion that has been lowered. For example, if the initial congestion is 4 MWh and the new congestion is 3 MWh then the Percentage reduce congestion will be 25%.
- The 3 rows below that hold the same type of data except it is for the number of hours where congestion occurs.
- Radial line 2 battery size: This shows the amount of battery capacity installed on the end of radial line 2. This location is the right most light blue block in Figure 5.1.
- Radial line 3 battery size: This shows the amount of battery capacity installed on the end of radial line 3. This location is the left most light blue block in Figure 5.1.
- Total price of battery: Costs of the total installation of the battery capacity.
- Curtailment costs: This is the amount of money it would cost to reimburse consumers in case load shedding is applied in order to eliminate the remaining congestion after the battery placement. The cost is determined by multiplying the remaining congestion with its correlating energy price. Thus the curtailment cost is the monetary value of the congestion causing energy.

From Tables 5.2 and 5.3 it is clear that the no constraint case is the better option. The percentage of congestion that is lowered is always higher for the no SOC setpoint constraint case. Only in 2036 the level of congestion reduction is higher for the 50% SOC setpoint constraint case. This can be explained by the fact that there is very little congestion in 2036, thus the scheduling of the battery has an increased importance. So the high percentage reduce congestion value for 2036 occurs, because of coincidence. This problem does not occur in later years, because of the increase in hours when congestion occurs and the law of large numbers.

The algorithms goal is to reduce the amount of congestion and not the number of times congestion occurs in the system. As explained in Figure 3.18 during its iterations the algorithm is capable of reducing the number of times congestion occurs, but it is also possible it will increase it instead. As shown in Tables 5.2 and 5.3, the hours when congestion occurs also lowers with the use of the energy arbitrage battery for both cases. While the 50% SOC setpoint constraint starts off with relieving 30% hours of congestion in 2036, it lowers through the years until it reaches 10 % in 2050. The hours of congestions

| Year | 2036 | 2038 | 2040 | 2042 | 2045 | 2050 |
|---|---|---|---|---|---|---|
| **Initial Congestion [MW]** | 5.84 | 95.71 | 244.08 | 395.27 | 525.20 | 716.52 |
| **New Congestion [MW]** | 3.54 | 77.57 | 193.95 | 331.12 | 436.65 | 605.3 |
| **Percentage reduced congestion [%]** | 39 | 19 | 21 | 16 | 17 | 15 |
| **Initial hours of congestion [h]** | 24 | 204 | 343 | 442 | 494 | 596 |
| **New hours of congestion [h]** | 17 | 156 | 280 | 378 | 428 | 537 |
| **percentage hours less [%]** | 29 | 24 | 18 | 14 | 13 | 10 |
| **Radial line 2 battery size [MWh]** | 4.25 | 4.25 | 6.5 | 6.5 | 6.8 | 7.5 |
| **Radial line 3 battery size [MWh]** | 0 | 0 | 0 | 0 | 0 | 1.15 |
| **Total price of battery [€]** | 807,500 | 807,500 | 1,223,750 | 1,223,750 | 1,274,750 | 1,515,000 |
| **Yearly curtailment costs [€]** | 267.62 | 5,212.7 | 12,858.89 | 21,688.36 | 28,513.25 | 39,465.56 |

**Table 5.2:** Results of the Optimal location and sizing. For the case when the battery uses the 50% end of day setpoint constraint which was discussed in Section 3.2.4

| Year | 2036 | 2038 | 2040 | 2042 | 2045 | 2050 |
|---|---|---|---|---|---|---|
| **Initial Congestion [MW]** | 5.84 | 96 | 244.08 | 395.27 | 525.2 | 716.52 |
| **New Congestion [MW]** | 4.66 | 75.3 | 186.7 | 292 | 384 | 522 |
| **Percentage reduced congestion [%]** | 20 | 21 | 24 | 26 | 27 | 27 |
| **Initial hours of congestion [h]** | 24 | 204 | 343 | 442 | 494 | 596 |
| **New hours of congestion [h]** | 17 | 147 | 245 | 312 | 346 | 433 |
| **percentage hours less [%]** | 29 | 28 | 29 | 29 | 30 | 27 |
| **Radial line 2 battery size [MWh]** | 2 | 4.15 | 6.95 | 8.05 | 10 | 10.65 |
| **Radial line 3 battery size [MWh]** | 0 | 0 | 0 | 0 | 0 | 1.15 |
| **Total price of battery [€]** | 380,000 | 777,750 | 1,281,750 | 1,479,750 | 1,711,250 | 1,829,000 |
| **Yearly curtailment costs [€]** | 352.3 | 5,060.16 | 12,378.21 | 19,126 | 25,075.2 | 34,034.4 |

**Table 5.3:** Results of the Optimal location and sizing. For the case when the battery has no SOC end of day setpoint constraint, which was discussed in Section 3.2.4

in the unconstrained case stay relatively stable around 29%.

This does come at a cost, because the amount of battery capacity that needs to be added to the network in order to hit the maximum congestion relief for the unconstrained case is higher than the constrained case. The unconstrained case has around 30% more battery capacity for most years, but it has 50% better performance in reducing congestion. This means that the extra investment is worth it.
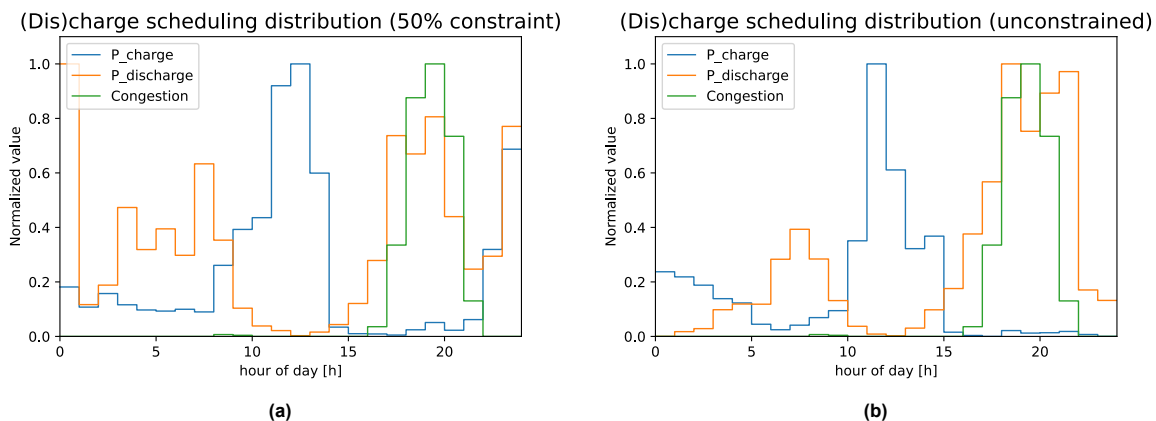


**Figure 5.5:** a) Shows the average distribution of battery and congestion of the time period 2020 - 2050 on a single day for the 50% SOC setpoint constraint. b) Shows the same, but for the unconstrained case.

Figure 5.5 shows the distribution of the charge and discharge scheduling of the battery and the

congestion. The two sub figures are very similar. To the left is the constrained case and to the right is the unconstrained case. Due to the 50% SOC setpoint the battery sometimes needs to make last hour corrections in order to reach the 50% SOC value at 24:00 o'clock. This results in the mixed charge and discharge amount at the last hour in Figure 5.5a. And because it starts at 50% SOC it is able to immediately discharge in case the early hours have cheap energy, which is also easy to see in the left of the figure. The unconstrained case is able to prioritize discharging all of its stored energy during the high demand times (16:00 - 22:00 o'clock). This explains why the unconstrained case preforms better.

### Sensitivity analysis

Figure 5.6 shows how the congestion changes as the amount of installed battery capacity of the algorithm changes for both cases. As can be seen, the congestion reduces as more battery capacity is added. After it found its optimal solution the congestion did not change anymore, because when the algorithm is not able to find a congestion reducing choice it will place battery capacity at the HV/MV substation, because there the charging and discharging will be absorbed by the external network, thus it will not cause any congestion. The installed battery capacity where the lowest amount of congestion is found, is represented in Figure 5.6 by blue dots. Also in Figures 5.6a&b it is easy to see that the unconstrained case has better results.
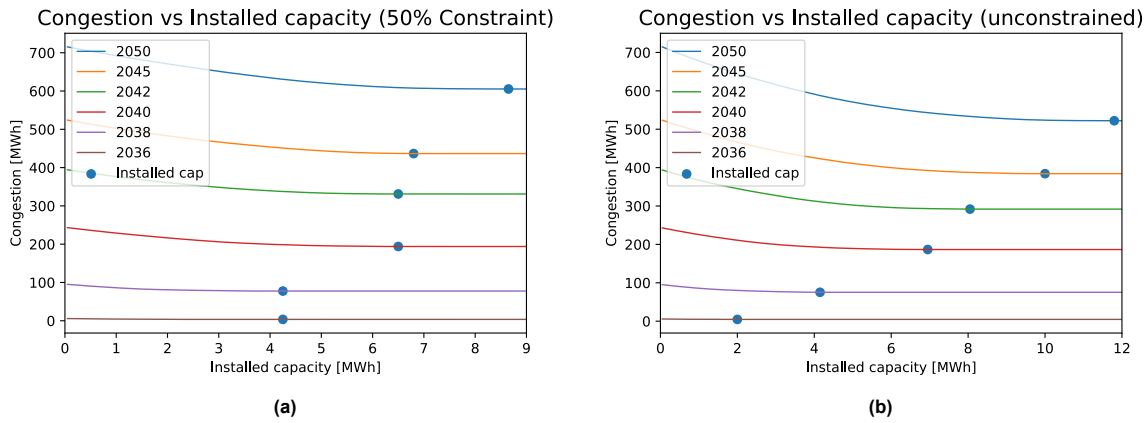


**Figure 5.6:** Figures a and b are both plots showing the effect of increasing the amount of installed battery capacity. The battery capacity is placed according to the algorithm. a) 50% SOC setpoint constraint case. b) unconstrained case.
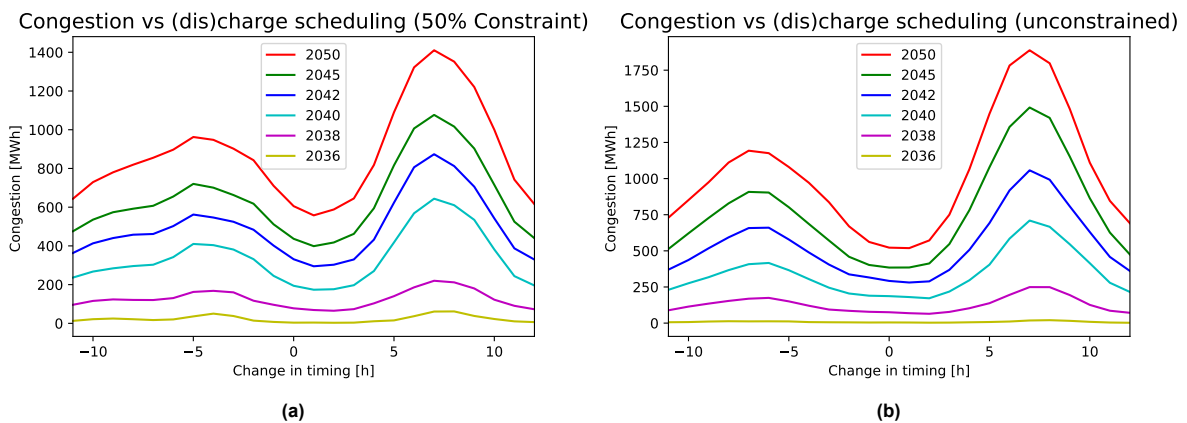


**Figure 5.7:** Sensitivity of the total congestion to changes in timing of the charging and discharging. In the positive direction it means that the charging and discharging happens one hour later, than the battery model decided. a) 50% SOC setpoint constraint case. b) unconstrained case.

Figure 5.7 shows, that when the scheduling of the energy arbitrage battery is changed, the conges-

tion is changed as well. It is interesting to note that the level of congestion relief is similar to the non changed case if the scheduling is changed by 12 hours. This can be explained by looking at Figure 5.5. For both cases there is a peak in discharge power between 17h and 21h and the other peak is between 5h and 9h. Between these two peaks there is exactly 12 hours and thus this secondary peak of discharging is reason for the relatively low congestion level on the sides of Figures 5.7a& b. The congestion level does not become lower than the congestion level in the middle of the figures. In this section it was shown that the 50% SOC setpoint constraint causes the congestion to worsen. So for the next cases, only the unconstrained results will be shown, but for those interested, the 50% SOC setpoint constraint cases of the Solar farm batteries and congestion relief cases are shown in Appendix A.

### 5.3.2.  Case: Solar farm batteries

In this case the same total battery capacity that was determined by the energy arbitrage algorithm was evenly distributed over the solar farms. This way the Solar farm batteries case can be easily compared to the Optimal Location and Size case. The rationale behind distributing battery capacity among solar farms is rooted in their suitability as potential battery installation sites. Solar farms are a probable choice due to their inherent volatility in energy production. Batteries can effectively store surplus energy generated by solar farms and release it when needed, thereby enhancing the overall efficiency of solar installations.

When the battery capacity from the optimal battery size is distributed over the solar farms, it is shown that the effect of the energy arbitrage is ineffective for this case study. This is because the batteries are mainly placed in radial lines that have no congestion as can be seen in Figure 5.1. For the solar farm installations inside of the grid. Radial line 1 and 2 have 1 solar farm each, Radial line 3 has 14 solar farms and Radial lines 4 and 5 have 2 solar farms each. The congestion mainly occurs on Radial line 2 and not on Radial line 3. The congestion in Radial line 3 only occurs in 2050. This means that unlike in the previous case, the battery installations will almost solely cause congestion.

| Year | 2036 | 2038 | 2040 | 2042 | 2045 | 2050 |
|---|---|---|---|---|---|---|
| Initial Congestion [MW] | 5.84 | 96 | 244.08 | 395.27 | 525.2 | 716.52 |
| New Congestion [MW] | 5.67 | 93.2 | 236.64 | 382.57 | 510.32 | 716 |
| Percentage reduced congestion [%] | 2.77 | 2.6 | 3 | 3.2 | 2.8 | 0.03 |
| Initial hours of congestion [h] | 24 | 204 | 343 | 442 | 494 | 596 |
| New hours of congestion [h] | 24 | 199 | 331 | 433 | 486 | 590 |
| Percentage hours less [%] | 0 | 2.51 | 3.32 | 2.08 | 1.65 | 0.85 |
| Radial line 2 battery size [MWh] | 0.11 | 0.22 | 0.37 | 0.42 | 0.53 | 0.62 |
| Radial line 3 battery size [MWh] | 1.47 | 3.06 | 5.12 | 5.93 | 7.37 | 8.69 |
| Total price of battery [€] | 380,000 | 777,750 | 1,281,750 | 1,479,750 | 1,711,250 | 1,829,000 |
| Yearly curtailment costs [€] | 441.5 | 6,444.48 | 16,148.69 | 25,901.32 | 34,295.56 | 51,534.08 |

**Table 5.4:** Results when battery capacity is evenly distributed over all solar farm locations. No SOC setpoint constraint

Table 5.4 shows that in 2036, 2038, 2040 and 2045 the total congestion and total hours of congestion both are reduced by around 3 percent. From 2050 onward the helpfulness of the battery installation is reduced. This is because, the increased load flow, that is caused by the charging of the batteries on Radial line 3, did not exceed the congestion limits until then. In the years before that, the only battery that had an effect was the single battery on Radial line 2.

### Sensitivity analysis

Figure 5.8a shows the sensitivity of the congestion to changes in the installed battery capacity. The blue circles show the chosen data points for the data from Table 5.4. The orange circles represent the maximum useful capacity for each respective year. If the installed capacity surpasses this threshold, the cumulative installations would exacerbate congestion instead of alleviating it. As can be seen the
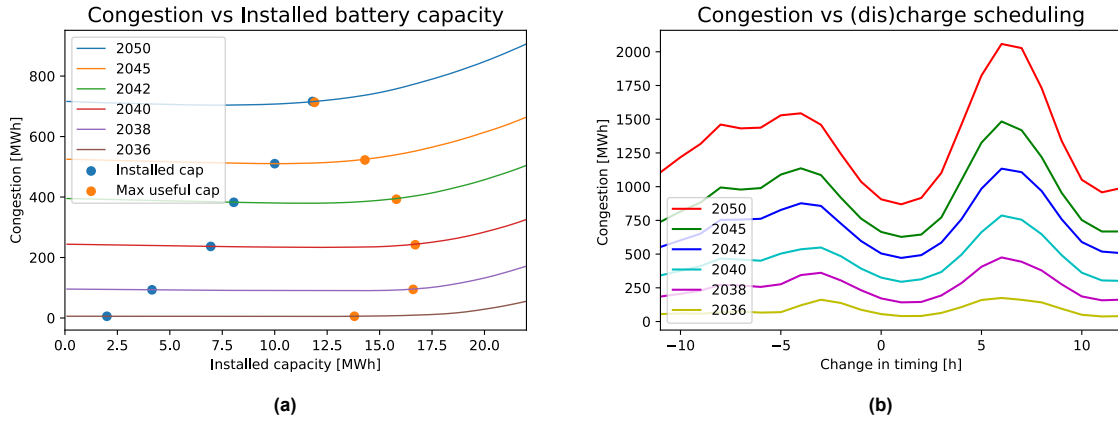
**Figure 5.8:** a) Sensitivity of the congestion to changes in the installed battery capacity. The blue circles show the chosen data points for the data from Table 5.4. The orange circles represent the maximum useful capacity for each respective year. If the installed capacity surpasses this threshold, the cumulative installations would exacerbate congestion instead of alleviating it. b) Sensitivity of the congestion to changes in the scheduling of the discharging and charging.

| Year | Maximum useful capacity limit |
|------|-------------------------------|
| **2036** | 13.8 |
| **2038** | 16.6 |
| **2040** | 16.7 |
| **2042** | 15.8 |
| **2045** | 14.3 |
| **2050** | 11.9 |

**Table 5.5:** Maximum useful capacity per year

result of 2050 is very close causing congestion, due to its proximity of the blue and orange circles. It is interesting to note that the maximum useful capacity becomes smaller as time goes on. The increasing demand throughout the years causes the power flow to come closer to the congestion limit. Thus, the threshold of charging power that is needed to reach the congestion limit is decreased as well.

In the years 2036 and 2038, the maximum useful capacity value is lower compared to that of 2040. This can be seen in Table 5.5. This disparity arises due to the greater influence of the battery on Radial line 2 during the earlier years. As this battery reaches its maximum useful capacity earlier than the batteries on Radial line 3, it leads to a reduction in the overall maximum useful capacity. However, in subsequent years, the impact of the single battery on Radial line 2 becomes less significant.

Figure 5.8b shows that changing the scheduling of discharging and charging will have a much lower effect compared to the optimal location and size case. From this it can be determined that by evenly distributing the battery capacity over the solar farms, the battery installation has an negligible effect on congestion, if its capacity is lower than the maximum useful capacity limit and if the capacity is higher than that it will start to cause congestion.

## 5.4. Congestion relief battery

The congestion relief battery is effective in reducing the congestion in the network. It retains this effectiveness from 2036 (99.6% congestion relief) up to 2050 (94% congestion relief) as can be seen in Table A.2. It is also more effective at reducing the number of hours where congestion occurs compared to the last two cases. This is because the congestion relief battery is not bound to a strict schedule for when to start discharging or charging. Due to this it is possible for the congestion relief battery to evade charging its battery in case its charging could cause congestion.

| Year | 2036 | 2038 | 2040 | 2042 | 2045 | 2050 |
|---|---|---|---|---|---|---|
| **Initial Congestion [MW]** | 5.84 | 96 | 244.08 | 395.27 | 525.2 | 716.52 |
| **New Congestion [MW]** | 0.03 | 5.7 | 6.93 | 18.69 | 19.07 | 41.5 |
| **Percentage reduced congestion [%]** | 99.6 | 94 | 97 | 95 | 96 | 94 |
| **Initial hours of congestion [h]** | 24 | 204 | 343 | 442 | 494 | 596 |
| **New hours of congestion [h]** | 2 | 21 | 26 | 45 | 42 | 63 |
| **Percentage hours less [%]** | 92 | 90 | 92 | 90 | 91 | 90 |
| **Radial line 2 battery size [MWh]** | 2 | 4.15 | 6.95 | 8.05 | 10 | 10.65 |
| **Radial line 3 battery size [MWh]** | 0 | 0 | 0 | 0 | 0 | 1.15 |
| **Total price of battery [€]** | 380,000 | 777,750 | 1,281,750 | 1,479,750 | 1,711,250 | 1,829,000 |
| **Yearly curtailment costs [€]** | 2.27 | 383.12 | 459.54 | 1,223.59 | 1,245.62 | 2,705.68 |

**Table 5.6:** Results for congestion relief

### 5.4.1. Sensitivity analysis

Figure 5.9 shows the sensitivity of the effectiveness of the congestion relief battery to the amount of its installed capacity. It shows that through the years it keeps taking more capacity in order to reduce the congestion to 0. Which is to be expected because of the increasing congestion through the years.
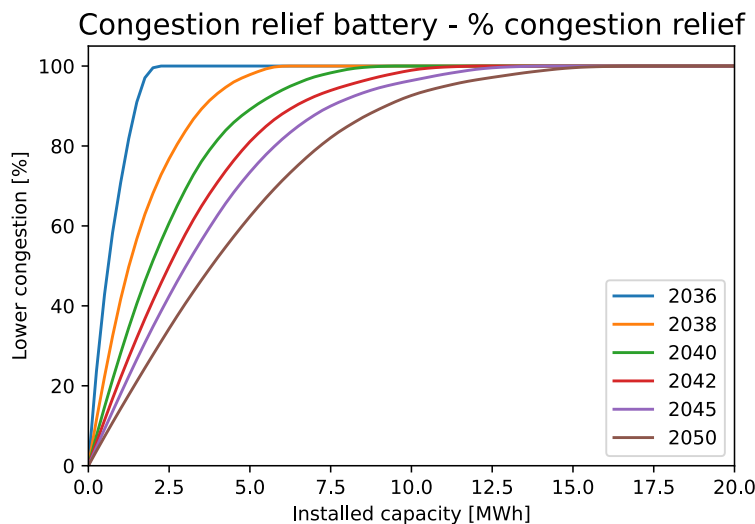


**Figure 5.9:** Sensitivity of congestion to installed congestion relief battery capacity.

## 5.5. Comparison

Figure 5.10a shows two important comparisons between the 3 cases. The installed capacity for these cases are equal to the optimally sized and located arbitrage battery. This way the different battery services are easy to compare.

Figure 5.10a & b show the difference in effectiveness in reduced congestion between the 3 cases. As can be seen the congestion relief battery is very effective and its results stay relatively stable at around 95%. The results for the arbitrage solar farm case show that it only has a small positibe effect on the congestion until the last year where it slightly worsens. This is due the energy arbitrage battery approaching the maximum useful capacity limit. Lastly the energy arbitrage that is optimally sized and located. This case increases in effectiveness as the years go on. This is caused by the increasing congestion. The congestion peak shown in Figure 5.5b will increase in size. Not only in amplitude, but also in its wideness. Consequently, the likelihood of congestion arising while the battery is discharging increases.
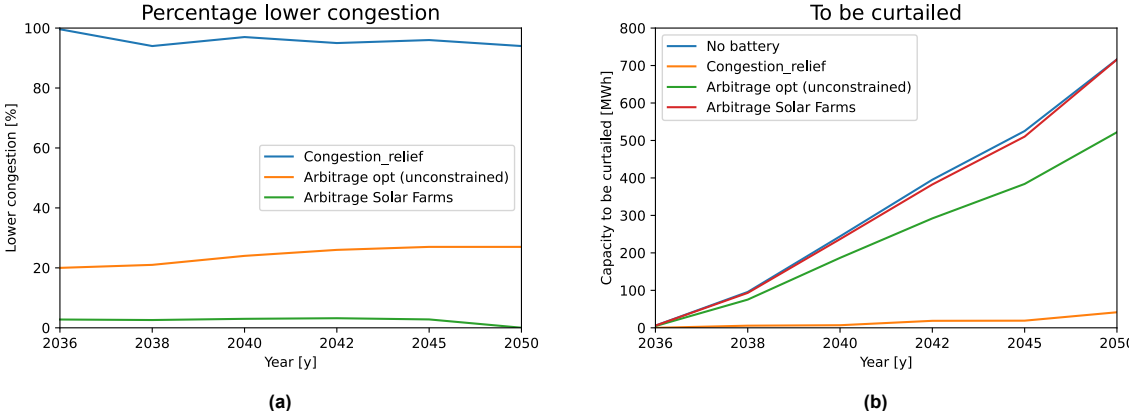
**Figure 5.10:** a) Percentage of congestion relief over the years. b) Amount of energy that is remaining the congestion limit after the batteries have been introduced and thus this needs to be curtailed.

# 6

# Conclusion and future work

Within this chapter, conclusions are derived from both the case study findings and the conducted research, thereby providing insights to address the research questions. After that, possible future work will be discussed.

## 6.1. Research questions

RQ1 - How can a strategically placed battery that uses energy arbitrage be used to relief congestion?

An energy arbitrage battery discharges when there is a high price and charges when there is a lower energy price. The price fluctuates throughout the day, but it has a repeating pattern. The congestion inside of the grid also follows a pattern. These patterns are shown in Figure 6.1.
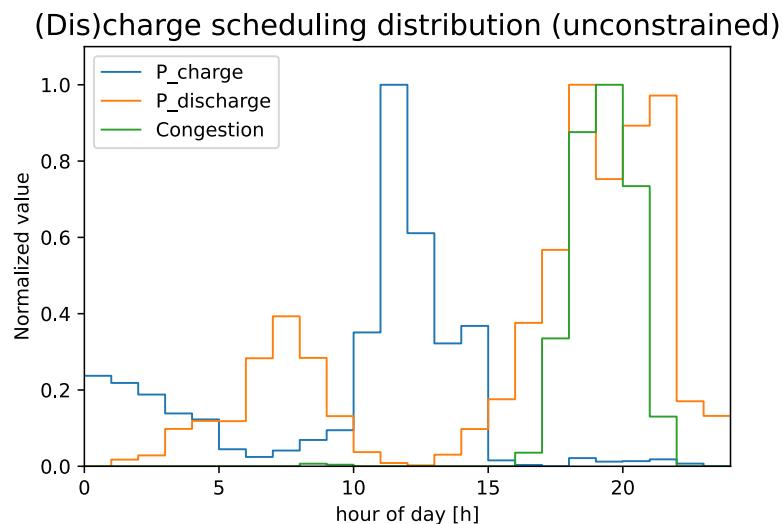


**Figure 6.1:** Comparison of discharge and charge scheduling distribution with the Congestion distribution.

As can be seen the congestion overlaps with the discharge times of the energy arbitrage battery. By placing the batteries in a location where, when the battery discharges, the congestion on a congested line reduces, it will result in the energy arbitrage battery having a net positive effect. For the case study, the congestion is reduced by 20% in 2036 and this beneficial effect progressively amplifies over the years, culminating in a 27% reduction in congestion relief by the final year, 2050. This increase in effectiveness is causes by the increase in congestion. As illustrated in Figure 6.1, the congestion peak expands not only in magnitude but also in duration. Consequently, the probability of congestion

coinciding with battery discharges rises..

RQ2 - What is the most effective location to add a battery in order to relieve congestion?
For this case study there is only one type of location that is the best location for the battery and that is the deepest part of the radial line. This is because of the losses that occur over the power lines. Equation 6.1 shows a general equation for the power flow through a radial line in case the power always flows from the outside grid towards the radial grid.

$$Power flow = (1 - Fraction_{Line\_loss}) * (Demand_{Radial} - Supply_{Radial}) \tag{6.1}$$

- $Power flow$: The amount of power that flows from the outside grid towards the radial line.
- $Fraction_{Line\_loss}$: Fraction of power that is lost while the power is flowing from the external grid towards the radial loads.
- $Demand_{Radial}$: The demand of the loads in the radial line.
- $Supply_{Radial}$: The supply of the generator in the radial line.

The equation shows that the power flow decreases in case of higher line losses and when the supply on the radial line increases. The location with the highest amount of losses is the deepest parts of the radial line, because the power needs to travel the furthest.

RQ3 - How do the most preferred location for the grid operator and the battery owner differ?
The grid operator prefers placing batteries at the end points of radial lines, while solar farm owners are the probable candidates for battery ownership. Given the volatility of solar farm energy production, it's highly likely that solar farm owners would possess batteries as well. These batteries are then placed next to or on the solar farm. This allows them to store excess energy generated by their solar farms for later use, leading to improved efficiency in their energy systems. As can been seen in Table 5.4, the energy arbitrage service is very ineffective in relieving congestion if the capacity is spread out over the solar farms.

RQ4 - How does battery storage compare to reinforcement of the grid when it comes to adding flexibility to the grid?
Energy system flexibility is the ability to adjust supply and demand to achieve the matching of supply and demand. Through the implementation of traditional grid reinforcement, the power cables' limits will not be reached within the simulated timeframe. The three outdated congested PILC cables in the case study network will be replaced with modern XLPE cables, leading to the peak power flow only reaching 87% of the congestion limit. Consequently, there is no longer need for quick reaction in order to reduce congestion inside of the grid. This means that the further need for flexibility is reduced in the case study network until 2050 at least. However it is not eliminated, because of the increase in solar power in the grid. This will introduce quick changing power flow. The increase in capacity of the power cables will not help in handling quickly changing supply and demand.

Both supply and demand can be adjusted with the help of batteries with the use of discharging and charging of the battery. Figure 5.9 shows that with the use of the congestion relief battery it is possible to completely eliminate the congestion in every year, if it has enough capacity installed. This means that the congestion relief battery is able to perform the flexibility task of the reinforcement option and because it is a battery, it is able to quickly react to power changes on solar farms. Hence, batteries offer greater flexibility to the grid compared to traditional reinforcement methods. However, to fully capitalize on this advantage, the battery's positioning and capacity are crucial. An ideal location should be chosen, and an appropriate capacity must be allocated for a significant impact. For instance, in the solar farm battery case, improper battery placement lead to congestion if the capacity became to big, while an inadequate capacity might result in negligible effects, as seen with the small battery in Radial line 2 in the solar farm batteries case.

RQ5 - How much better is a congestion relief service providing battery at relieving congestion compared to the battery that uses energy arbitrage.
In order to make an equal comparison the total capacities of all battery options are kept the same as the Optimal location and size case with the unconstrained SOC setpoint of the energy arbitrage option.

Figure 5.10a shows the difference in congestion relief. It is clear that the congestion relief battery performs around 4 times better compared to the optimally located and sized version of the energy arbitrage battery. For the solar farm batteries case the results show that it is ineffective at reducing congestion.

RQ6 - To what extent will load curtailment be needed, when batteries are introduced to the system instead of reinforcing the grid?
Curtailment will be needed in case energy arbitrage batteries are used. This is due to the batteries not prioritizing lower congestion. While it is able to reduce congestion on certain hours of the day, namely the hours when it is decided that it will start to discharge. For this case, load curtailment becomes necessary to reduce congestion to the cable's limit. In the case of the optimally sized and located option, in 2036, a curtailment of 80% of the initial congestion is required. This curtailment decreases over the years, reaching 73% by 2050. In contrast, for the solar farm battery case, curtailment of 97% is necessary, with the exception of 2050 where it reaches 99%.

In contrast to energy arbitrage batteries, congestion relief batteries possess the potential to completely eradicate congestion when equipped with sufficient capacity. If the total installed capacity matches that of the optimally sized and located energy arbitrage battery, the congestion relief battery only needs to curtail approximately 5% of the initial congestion.

## 6.2. Final thoughts
Through this research it is possible to say that energy arbitrage batteries are able to be used in a net positive way. The most important part for this is the location. In the case of the radial grid, the congestion causing cable should be in between the energy arbitrage battery and the external grid and the congestion should be large enough. If the congestion in the line is very small, it could result in more congestion when the energy arbitrage battery is large enough as could be seen in the solar farm case.

However, while energy arbitrage batteries can offer a positive impact, relying solely on them as a solution is insufficient; they necessitate support from complementary technologies such as load curtailment, for instance.

## 6.3. Future work
While this study has provided valuable insights into the effectiveness of energy arbitrage batteries as congestion relief batteries, several openings for future research remain unexplored.

Due to a lack of data it was not possible to model the intra-day market. This resulted in a relatively simple market model, that could be improved upon in order to make it more realistic. With the current market model the price could stay constant for multiple hours in a row, which is not representative of the real energy market.

As explained in Section 5.5 the effectiveness of the energy arbitrage battery increases throughout the years due to the increasing congestion. If the simulation data goes further into the future, it can be found how much more effective the battery can become or if the effectiveness starts to degrade early after the year 2050.

In this thesis, multiple different options for congestion relief are looked into and compared. An interesting possible future research direction will be researching what the optimal mix will be of traditional reinforcement, energy arbitrage, congestion relief or curtailment.

The network of the case study is fully radial. This made finding the optimal location in the network simple. It will be interesting to look into how the results will change if the network were to be meshed.

# References

1. *The Paris Agreement* `https://unfccc.int/process-and-meetings/the-paris-agreement/the-paris-agreement`.

2. *Grootverbruikers van elektriciteit in Noord-Brabant en Limburg kunnen vanaf nu weer worden aangesloten* nl. `https://www.tennet.eu/nl/nieuws/grootverbruikers-van-elektriciteit-noord-brabant-en-limburg-kunnen-vanaf-nu-weer-worden` (2023).

3. *Stedin sluit alleen onder voorwaarden batterijexploitanten aan* en. `https://www.stedin.net/over-stedin/pers-en-media/persberichten/stedin-sluit-alleen-onder-voorwaarden-batterijexploitanten-aan` (2023).

4. Wogrin, S. & Gayme, D. F. Optimizing Storage Siting, Sizing, and Technology Portfolios in Transmission-Constrained Networks. *IEEE Transactions on Power Systems* **30,** 3304–3313. ISSN: 1558-0679 (Nov. 2015).

5. Van Westering, W. & Hellendoorn, H. Low voltage power grid congestion reduction using a community battery: Design principles, control and experimental validation. en. *International Journal of Electrical Power & Energy Systems* **114,** 105349. ISSN: 0142-0615. `https://www.sciencedirect.com/science/article/pii/S0142061519305009` (2023) (Jan. 2020).

6. Van Westering, W. & Hellendoorn, H. Low voltage power grid congestion reduction using a community battery: Design principles, control and experimental validation. en. *International Journal of Electrical Power & Energy Systems* **114,** 105349. ISSN: 0142-0615. `https://www.sciencedirect.com/science/article/pii/S0142061519305009` (2023) (Jan. 2020).

7. Rietveld, J. Optimising BESS Control Strategies for Congestion and Price Arbitrage. en. `https://repository.tudelft.nl/islandora/object/uuid%5C%3A35e85746-328f-45d3-bab5-2f1c16bbad35` (2023) (2022).

8. Kers, B. *Ontwerp middenspanningsnetten STEDIN* Dutch. 2022.

9. *warmtegeleidingscoefficient lambda* `https://www.joostdevree.nl/shtmls/warmtegeleidingscoefficient.shtml` (2023).

10. *Ondergrondmodellen | DINOloket* `https://www.dinoloket.nl/ondergrondmodellen/kaart` (2023).

11. *GisWeb 2.2 - Grondwater* `https://www.gis.rotterdam.nl/Gisweb2/Default.aspx?context=MIJNPROJECT.1091` (2023).

12. *PowerFactory - DIgSILENT* `https://www.digsilent.de/en/powerfactory.html` (2023).

13. Sood, P., Tylavsky, D., Vittal, V. & Ayyanar, R. *Development of Improved dc Network Model for Contingency Analysis CORE View metadata, citation and similar papers at core.ac.uk provided by ASU Digital Repository* (2014).

14. Bierling, P. *Creating a coupling and synergy between SETIAM and Netrekenen models* Company presentation. Stedin, 2022.

15. *Market Data | EPEX SPOT* `https://www.epexspot.com/en/market-data` (2023).

16. Schavemaker, P. & Sluis, L. *Electrical Power System Essentials* ISBN: 978-0-470-51027-8 (Apr. 2008).

17. *Over GOPACS* nl. `https://www.gopacs.eu/over-gopacs/` (2023).

18. *Home - ETPA* nl. `https://www.etpa.nl/nl/` (2023).

19. Müsgens, F., Ockenfels, A. & Peek, M. Economics and design of balancing power markets in Germany. en. *International Journal of Electrical Power & Energy Systems* **55,** 392–401. ISSN: 0142-0615. `https://www.sciencedirect.com/science/article/pii/S014206151300402X` (2023) (Feb. 2014).

20. *Our high voltage grid* nl. `https://content.tennet.eu/nl/node/1262` (2023).

21. Siemensma, R. *Energy Storage System Modelling - Modelling the influence of large-scale profit optimisingenergy storage systems participating in both energy andbalancing markets* English. PhD thesis (T.U. Delft, Delft, 2022).

22. Ehrenmann, A. *The future electricity intraday market design* English. 2019. `https://eepublicd ownloads.entsoe.eu/clean-documents/Network%5C%20codes%5C%20documents/Implementat ion/stakeholder_committees/MESC/2019-09-17/190917_5.8_EC%5C%20study%5C%20on%5C% 20ID%5C%20market%5C%20design.pdf?Web=1`.

23. Zhao, H., Hong, M., Lin, W. & Loparo, K. A. Voltage and Frequency Regulation of Microgrid With Battery Energy Storage Systems. *IEEE Transactions on Smart Grid* **10,** 414–424. ISSN: 1949-3061 (Jan. 2019).

24. Khatibi, M. & Ahmed, S. *Impact of Distributed Energy Resources on Frequency Regulation of the Bulk Power System* in *2019 IEEE Conference on Power Electronics and Renewable Energy (CPERE)* (Oct. 2019), 258–263.

25. Gunturu, R. S. S. *Forecasting Intraday Electricity Market Prices: Deep Learning vs Traditional Approaches Declaration concerning the TU/e Code of Scientific Conduct for the Master's thesis* (2020). `https://www.tue.nl/en/our-university/about-the-university/organization/ integrity/scientific-integrity/`.

26. Kath, C. Modeling Intraday Markets under the New Advances of the Cross-Border Intraday Project (XBID): Evidence from the German Intraday Market. en. *Energies* **12,** 4339. ISSN: 1996-1073. `https://www.mdpi.com/1996-1073/12/22/4339` (2023) (Nov. 2019).

27. Dresden, T. U., Society, I. P. bibinitperiod E., of Electrical, I. & Engineers, E. *2017 14th International Conference on the European Energy Market (EEM) : 6-9 June 2017, Dresden, Germany* ISBN: 9781509054992 ().

28. Oksuz, I. & Ugurlu, U. Neural Network Based Model Comparison for Intraday Electricity Price Forecasting. en. *Energies* **12,** 4557. ISSN: 1996-1073. `https://www.mdpi.com/1996-1073/12/ 23/4557` (2023) (Nov. 2019).

29. *ENTSO-E Transparency Platform* `https://transparency.entsoe.eu/` (2023).

30. Afman, M. & Kellner, M. *Integrale Energiesysteemverkenning 2030 - 2050* webinar 5 (Netbeheer Nederland, 2023), 57.

31. Afman, M. & Kellner, M. *Integrale Energiesysteemverkenning 2030 - 2050* Jan. 2023.

32. Zaken, M. v. A. *België en Nederland gaan meer samenwerken op vlak van veiligheid en energieomslag - Nieuwsbericht - Rijksoverheid.nl* nl-NL. nieuwsbericht. Apr. 2022. `https://www. rijksoverheid.nl/actueel/nieuws/2022/04/19/belgie-en-nederland-gaan-meer- samenwerken-op-vlak-van-veiligheid-en-energieomslag` (2023).

33. *Internationale samenwerking voor windenergie op zee* nl. `https://www.rvo.nl/onderwerpen/ windenergie-op-zee/internationale-samenwerking` (2023).

34. *Internationale samenwerking zonne-energie* nl. `https://www.rvo.nl/onderwerpen/zonne- energie/internationale-samenwerking` (2023).

35. Global Modeling And Assimilation Office & Pawson, Steven. *MERRA-2 inst1_2d_asm_Nx: 2d,3-Hourly,Instantaneous,Single-Level,Assimilation,Single-Level Diagnostics V5.12.4* Type: dataset. 2015. `https://disc.gsfc.nasa.gov/datacollection/M2I1NXASM_5.12.4.html` (2023).

36. *Renewables.ninja* `https://www.renewables.ninja/` (2023).

37. Zaken, M. v. A. *Borssele voorkeurslocatie voor twee nieuwe kerncentrales - Nieuwsbericht - Rijksoverheid.nl* nl-NL. nieuwsbericht. Dec. 2022. `https://www.rijksoverheid.nl/actueel/ nieuws/2022/12/09/borssele-voorkeurslocatie-voor-twee-nieuwe-kerncentrales` (2023).

38. *Press corner* en. Text. `https://ec.europa.eu/commission/presscorner/home/en` (2023).

39. *Power plants: Hemweg 9 - a new gas fired plant - Vattenfall* `https://powerplants.vattenfall. com/hemweg-9/` (2023).

40. *Toekomstscenarios - Netbeheer Nederland* `https://www.netbeheernederland.nldossiers/` `toekomstscenarios-64` (2023).

41. *Energy market - Energie Nederland* en-US. `https://www.energie-nederland.nl/en/facts-` `figures/energy-market/` (2023).

42. *LCOE range for selected dispatchable low emissions electricity sources in the Sustainable Development Scenario, 2030, 2040 and 2050 – Charts – Data & Statistics* en-GB. `https://www.` `iea.org/data-and-statistics/charts/lcoe-range-for-selected-dispatchable-low-` `emissions-electricity-sources-in-the-sustainable-development-scenario-2030-2040-` `and-2050` (2023).

43. Badouard, T. *Final report cost of energy (LCOE)* English. Report (Trinomics, 2020), 62. `https:` `//energy.ec.europa.eu/system/files/2020-10/final_report_levelised_costs_0.pdf`.

44. *Levelised Cost of Electricity Calculator – Data Tools* en-GB. `https://www.iea.org/data-and-` `statistics/data-tools/levelised-cost-of-electricity-calculator` (2023).

45. Sens, L., Neuling, U. & Kaltschmitt, M. Capital expenditure and levelized cost of electricity of photovoltaic plants and wind turbines – Development by 2050. *Renewable Energy* **185,** 525–537. ISSN: 18790682 (Feb. 2022).

46. Wiser, R. *et al.* Expert elicitation survey predicts 37% to 49% declines in wind energy costs by 2050. *Nature Energy* **6,** 555–565. ISSN: 20587546 (5 May 2021).

47. *The Leader in Decision Intelligence Technology* en-US. `https://www.gurobi.com/` (2023).

48. *Basics of the Power Market | EPEX SPOT* `https://www.epexspot.com/en/basicspowermarke` `t#day-ahead-and-intraday-the-backbone-of-the-european-spot-market` (2023).

49. Moura, S., Chaturvedi, N. & Krstić, M. Adaptive Partial Differential Equation Observer for Battery State-of-Charge/State-of-Health Estimation Via an Electrochemical Model. *Journal of Dynamic Systems, Measurement, and Control* **136,** 011015 (Oct. 2013).

50. Ghavamzadeh, M., Petrik, M. & Chow, Y. *Safe Policy Improvement by Minimizing Robust Baseline Regret* in *Advances in Neural Information Processing Systems* (eds Lee, D., Sugiyama, M., Luxburg, U., Guyon, I. & Garnett, R.) **29** (Curran Associates, Inc., 2016). `https://proceedings.` `neurips.cc/paper_files/paper/2016/file/9a3d458322d70046f63dfd8b0153ece4-Paper.` `pdf`.

51. Møller, K. T., Jensen, T. R., Akiba, E. & wen Li, H. Hydrogen - A sustainable energy carrier. *Progress in Natural Science: Materials International* **27,** 34–40. ISSN: 17455391 (1 Feb. 2017).

52. Kousksou, T., Bruel, P., Jamil, A., Rhafiki, T. E. & Zeraouli, Y. *Energy storage: Applications and challenges* 2014.

53. Schmidt, O., Melchior, S., Hawkes, A. & Staffell, I. Projecting the Future Levelized Cost of Electricity Storage Technologies. *Joule* **3,** 81–100. ISSN: 25424351 (1 Jan. 2019).

54. Hugenholtz, D. E. *Batteries and energy arbitrage A techno-economic analysis of electricity arbitrage opportunities for utility-scale battery energy storage in the Netherlands* (). `www.pexels.com.`.

55. Cole, W. & Frazier, A. *Cost Projections for Utility-Scale Battery Storage: 2020 Update,* Tech. Rep. (NREL, 2020).

56. Zhao, B., Member, S., Conejo, A. J., Sioshansi, R. & Member, S. *IEEE TRANSACTIONS ON POWER SYSTEMS 1 Using Electrical Energy Storage to Mitigate Natural Gas-Supply Shortages* (). `http://www.cpuc.ca.gov/Aliso`.

57. Arroyo, J. M. *et al.* On the Use of a Convex Model for Bulk Storage in MIP-Based Power System Operation and Planning. *IEEE Transactions on Power Systems* **35,** 4964–4967. ISSN: 15580679 (6 Nov. 2020).

58. Pozo, D. Linear Battery Models for Power Systems Analysis. `http://arxiv.org/abs/2204.` `08240` (Apr. 2022).

59. Stecca, M., Elizondo, L. R., Soeiro, T. B., Bauer, P. & Palensky, P. *A comprehensive review of the integration of battery energy storage systems into distribution networks* 2020.

60.  Jiang, J. *et al.* Optimized Operating Range for Large-Format LiFePO 4 /Graphite Batteries. *Journal of The Electrochemical Society* **161,** A336–A341. ISSN: 0013-4651 (3 2014).

61.  Simmons, B. I., Hoeppke, C. & Sutherland, W. J. *Beware greedy algorithms* May 2019.

62.  Bowen, T., Chernyakhovskiy, I. & Denholm, P. *Grid-Scale Battery Storage: Frequently Asked Questions* (). `www.greeningthegrid.org`.

63.  DIgSILENT. *User Manual* (2019).

# A
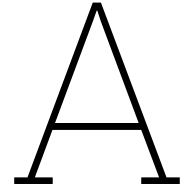
## 50% SOC setpoint constraints cases results

### A.1. Case: Solar farm batteries

| Year | 2036 | 2038 | 2040 | 2042 | 2045 | 2050 |
|---|---|---|---|---|---|---|
| Initial Congestion [MW] | 5.84 | 96 | 244.08 | 395.27 | 525.2 | 716.52 |
| New Congestion [MW] | 5.8 | 95.8 | 243.93 | 395.08 | 525.1 | 724.68 |
| Percentage reduced congestion [%] | 0.7 | 0.1 | 0.06 | 0.05 | 0.01 | -1.14 |
| Initial hours of congestion [h] | 24 | 204 | 343 | 442 | 494 | 596 |
| New hours of congestion [h] | 23 | 200 | 336 | 438 | 492 | 592 |
| Percentage hours less [%] | 4.35 | 2 | 1.79 | 0.9 | 0.4 | 0.5 |
| Radial line 2 battery size [MWh] | 0.22 | 0.22 | 0.34 | 0.34 | 0.36 | 0.46 |
| Radial line 3 battery size [MWh] | 3.08 | 3.08 | 4.76 | 4.76 | 5.04 | 6.37 |
| Total price of battery [€] | 807,500 | 807,500 | 1,223,750 | 1,223,750 | 1,274,750 | 1,515,000 |
| Yearly curtailment costs [€] | 438.48 | 6,410.88 | 16,165.27 | 25,861.37 | 34,285.77 | 46,661.03 |

**Table A.1:** Results when battery capacity is evenly distributed over all solar farm locations. 50% SOC setpoint constraint

### A.2. Case: Congestion relief battery

| Year | 2036 | 2038 | 2040 | 2042 | 2045 | 2050 |
|---|---|---|---|---|---|---|
| Initial Congestion [MW] | 5.84 | 96 | 244.08 | 395.27 | 525.2 | 716.52 |
| New Congestion [MW] | 0 | 7 | 10 | 40 | 70 | 130 |
| Percentage reduced congestion [%] | 100 | 92 | 96 | 90 | 87 | 82 |
| Initial hours of congestion [h] | 24 | 204 | 343 | 442 | 494 | 596 |
| New hours of congestion [h] | 0 | 25 | 35 | 81 | 130 | 214 |
| percentage hours less [%] | 100 | 88 | 90 | 82 | 74 | 65 |
| Radial line 2 battery size [MWh] | 4.25 | 3.9 | 6.5 | 6.4 | 6.8 | 7.5 |
| Radial line 3 battery size [MWh] | 0 | 0 | 0 | 0 | 0 | 1.15 |
| Total price of battery [€] | 807,500 | 807,500 | 1,223,750 | 1,223,750 | 1,274,750 | 1,515,000 |
| Yearly curtailment costs [€] | 0 | 470.4 | 663 | 2,620 | 4,571 | 8,476 |

**Table A.2:** Results when battery is a congestion relief battery and uses the battery distribution of the Case: Optimal Location and Size